Journal of Hydrology 626 (2023) 130213

Contents lists available at ScienceDirect

Journal of Hydrology

journal homepage: www.elsevier.com/locate/jhydrol

Research papers

A holistic approach for using global climate model (GCM) outputs in decision making

Sanjeewa Illangasingha [a,b,*], Toshio Koike [a,b], Mohamed Rasmy [a,b], Katsunori Tamakawa [a], Hirotada Matsuki [c], Hemakanth Selvarajah [d]

[a] International Centre for Water Hazard and Risk Management (ICHARM), Public Works Research Institute, Japan
[b] National Graduate Institute for Policy Studies (GRIPS), Japan
[c] National Institute for Land and Infrastructure Management (NILIM), Japan
[d] Del & Dee Ltd, United Kingdom

ARTICLE INFO

This manuscript was handled by Emmanouil Anagnostou, Editor-in-Chief, with the assistance of Viviana Maggioni, Associate Editor.

Keywords:
Uncertainty
Climate change
General circulation models
Seasonal climate variables
Degree of confidence
Decision-making

ABSTRACT

All human endeavours are affected by climate change and local weather, and 21st-century climate-change estimates will provide greater challenges. Therefore, numerical model-based climate projections (i.e., General Circulation Models – GCMs) are essential for making decisions about adaptation, mitigation, and resilience building to combat adverse climate impacts. However, these coarser resolution model projections have uncertainties resulting in significant doubts in decision-making, particularly in the local or regional domain. Thus, we suggest five principles for GCM use at local and regional scales to overcome uncertainties in decision-making. This study examines historical and projected precipitation from 44 GCMs, calculated under the Representative Concentration Pathways (RCP) 8.5 scenario considering regional, geographical, and temporal variability for establishing a decision-making support system based on the degree of confidence for nine diverse main river basins in tropical Sri Lanka as a case study. Each GCM confirmed the current climatic pattern in terms of wind vector and meridional wind patterns out of eight climate variables considered. GCM sensitivity varies geographically and temporally. An annual precipitation study is not enough to make climate change judgments because climate change signals change seasonally. Each basin's average annual precipitation was projected to likely increase over the near, middle, and far future (2025–2050, 2050–2075, 2075–2100, respectively); however, in the Mahaweli basin (MB), the largest basin neighboring most of the other basins, the annual precipitation was projected to extremely likely increase. Most of MB's surrounding basins show a more-likely-than-not decreasing precipitation tendency for inter-monsoon-1 in the future (2025–2100); however, MB shows a more-likely-than-not increasing trend. Our analysis shows that the southwest monsoon and inter-monsoon-2 are more likely than not or extremely likely to strengthen, whereas the northeast monsoon (NEM) and inter-monsoon-1 are more likely than not to weaken, excluding NEM in the near future. Here, we introduced a simple color-coded climate change (C4) matrix for decision-making that provides spatial, temporal, and seasonal climate change projections likelihood trends with current observed seasonal trends. Future projections indicate a swapping in seasonal precipitation trends between IM-1 and SWM for almost basins compared to the past. NEM appears to have a weakening influence on the majority of northeast-facing basins during the middle and far future. A simple detailed climate analysis chart may be more effective in communicating scientific messages to the scientific community and the key public actors who make decisions.

1. Introduction

1.1. Background

Long-term climate change trends and local weather phenomena are crucial factors affecting all human endeavours (Gitz et al., 2016). Foreshadowed climate-change projections for the 21st century are certain to pose additional challenges to society. Thus, human well-being in the future is indivisibly connected to our ability to manage the hazards associated with climatic variability (IPCC, 2013). In this regard,

* Corresponding author at: International Centre for Water Hazard and Risk, Management (ICHARM), Public Work Research Institute, 1-6 Minamihara, Tsukuba, Ibaraki, Japan.
E-mail address: sanjeesri@gmail.com (S. Illangasingha).

https://doi.org/10.1016/j.jhydrol.2023.130213
Received 9 May 2023; Received in revised form 29 August 2023; Accepted 1 September 2023
Available online 28 September 2023

decision-makers require climate services to help implement adaptation and mitigation measures against climate change-induced consequences, such as droughts, heat waves, floods, landslides, and coastline erosion. However, climate service-based decision-making should accommodate key uncertainties originating from, for example, models, climate zones, and temporal changes, as described in the following paragraphs.

Climate explains the long-term weather trend in a particular region in contrast to the weather, which describes short-term variations in the atmosphere. People have investigated several methods to study the earth's climate system for better and more resilient living standards. Weather and climate models refer to a numerical representation of the climate system based on the physical, chemical, and biological aspects of its components, as well as their interactions and feedback processes (Dierickx, 2019; Hannah, 2015; Stocker, 2016). However, they differ in distinct ways (Dierickx, 2019; Stocker, 2016). Weather models perform simulations with relatively short lead times (up to 15 days). On the other hand, climate models make predictions for more extended periods, such as hundreds of years, and are more concerned with long-term statistics than when and where relevant events (i.e., weather fronts) occur (Dierickx, 2019; Randall et al., 2007). The design and maintenance of infrastructure, as well as emergency response management and long-term investment and planning, are all underpinned by assumptions on stationarity and non-stationarity (Kotamarthi et al., 2016). Climate, as a result, is crucially significant, and the outputs of climate models play a vital role in decision-making tasks (Kotamarthi et al., 2016). In the past 20 years, there have been significant advancements in both the development of climate models and their applications, and the models that are currently in use provide us with reliable indications that future climate change may vary (Randall et al., 2007). However, climate models contain several uncertainties, representing the deviation from the unattainable ideal of absolute determinism (Hawkins and Sutton, 2009; Walker et al., 2003). These uncertainties virtually affect every aspect of policymaking (Walker et al., 2003).

Three different types of uncertainty can be identified in climate projections: Natural variability, scenario uncertainty, and model uncertainty (Hawkins and Sutton, 2009; Walker et al., 2003). Natural variability is caused by interactions among climate system components, occurs in the absence of any radiative force on the globe, and can be periodic, random, or chaotic (Hawkins and Sutton, 2009; Kotamarthi et al., 2016). However, while it substantially affects the overall uncertainty of near-future projections (e.g., precipitation), its contribution to middle- or far-future projections is comparatively much less than model uncertainty (Hawkins and Sutton, 2009; Raisanen, 2001). Scenario uncertainty is the uncertainty in future greenhouse gas emissions caused by natural and human activities and the concentration of scenarios. The range of emissions depends not only on natural actors and human actions but also on present decisions, policy implementations, modifications, and changes (Hawkins and Sutton, 2009; Kotamarthi et al., 2016; Solomon et al., 2007). Model uncertainty refers to the slightly varying responses (projections) of different models to the same radiative forcing induced by the model's own built structures (Hawkins and Sutton, 2009; Walker et al., 2003). General circulation models (GCMs) are one type of climate model. Since climate models include atmospheric and oceanic processes, they should integrate over a much longer time than weather prediction models. They also require a large amount of computational load and capacity and cannot use a fine resolution as the climatic system becomes complex. As a result, GCMs that use coarse resolutions cause considerable uncertainty. Interaction processes, such as cloud, radiative, and boundary-layer processes of the climate system, are not resolved adequately due to the climate models' limitations in grid resolution and computational capability. Therefore, simplifying those processes in climate models' parameterisation has been introduced (Mcfarlane, 2011; Randall et al., 2007). GCMs incorporate a range of physical processes; these processes are also parametrised. GCMs employ various simplification and approximation methodologies based on model consideration, resolution, and computer capacity. As a result, the model uncertainty in GCMs varies (Leung et al., 2013; Mcfarlane, 2011). Model uncertainty influences the overall uncertainty of the projections over longer timescales. The contribution of uncertainty in the mid or far future is more significant than other types of uncertainties (Hawkins and Sutton, 2009). With the advancement of research over the last decade, the resolution of the GCMs employed in the Coupled Model Intercomparison Project phase 6 (CMIP6) project has seen some improvement, resulting in considerably reduced uncertainty at the global scale. However, at regional and local scales, there is still significant uncertainty within the projections (IPCC, 2021).

Due to the uncertainties in GCMs, certain GCMs may not reproduce the current regional or local climate and have discrepancies. Thus, using these GCMs for decision-making may generate doubts in scientific and public communities. There is uncertainty when utilising (downscaling) GCMs for regional or local projections since they have a significantly coarser resolution and localised atmospheric processes, topography, and other geographic characteristics that are not fully addressed by climate models (Kotamarthi et al., 2016). Climate sensitivity is the aggregate outcome of a wide range of feedback mechanisms in the climate system, making it difficult to explain the precise relationship and contribution over an extended period, regardless of whether models with high or low climate sensitivities for projections (Mauritzen et al., 2017; Räihä, 2019). It is a significant source of model uncertainty for major climate variable projections such as precipitation, temperature, and wind over a large global region (Mauritzen et al., 2017). The projection's climate sensitivity range should be confirmed to make acceptable conclusions. Also, confidence analysis of GCMs' sensitivity can help policymakers make sound decisions because such analysis gives them more confidence in how sensitive GCMs are (Solomon et al., 2007).

There are only a limited number of studies on the uncertainty of climatic change inter-comparison for local areas in the same region with diverse hydrologic circumstances such as affecting tropical climate, monsoon, and different types of basins. Furthermore, different basins in the same region depend on water-related agriculture or other industries, and different types of water-related disasters, such as floods, droughts, and landslides. They also behave as in individual or interconnected water-related societies. Therefore, we have chosen diverse climatic regions to respond to the scientific issues we need to resolve. The reasoning for this choice comes from the need for further scientific clarifications regarding the diversity of the climate of the different areas in the same region. For example, in this study, we focus on addressing the uncertainty mentioned above at regional and local scales with various climatic zones. Some regions are dry, while others are wet, and there is a significant variation in the seasonal climate. Even in dry regions, some seasons are wet, while others have a long dry season. Furthermore, various mechanisms influence monsoon rainfall, and because of topography, monsoonal effects vary between local areas. If we choose such an area, we can handle the diversity and variability while attempting to find an approach for addressing (quantifying) uncertainty at the regional and local levels. In order to handle the uncertainty mentioned above, we need to develop an approach. In order to achieve this goal, we have to choose a region and scientific research subject to develop an acceptable decision-making system.

Therefore, developing new approaches to resolving key uncertainties, such as those related to models, climate zones, and temporal changes, is vital. Accordingly, we propose five principles for using GCMs at the regional or local scale to address the uncertainties mentioned above in decision-making: 1) The climate models used for decision-making should accurately represent the current regional climate; 2) When using GCMs at the regional or local scale, downscaling and bias correction should be implemented; 3) The climatic sensitivity of climate models should be identified; 4) The discrepancies in outcomes among climate models should be understood; and 5) Climate models should be able to address diverse environments. The following sections describe available methods, technologies, and tools for addressing the above five principles and developing a framework for employing GCMs in decision-

making.

Temperature and precipitation are the key parameters for assessing climate change impacts on the water cycle. Temperature influences the evapotranspiration process, which is a relatively longer-term phenomenon that has a substantial impact on water resource management. "All regions are projected to experience further increases in hot climatic" (IPCC, 2021). Global climate system warming is unequivocal (IPCC, 2021), thus leading to myriad changes in the atmosphere and water cycle. Climate change is affecting every inhabited region globally. Human influence is evident in observed weather and climate extremes, especially hot extremes in some regions. However, attributing heavy precipitation to human-induced climate change remains uncertain, with low confidence compared to temperature changes (IPCC, 2021). Regarding the temperature of GCMs, the increase rate has no significant uncertainty at the global and regional scale for all greenhouse emission scenarios (IPCC, 2021). However, precipitation projections still have significant uncertainty and are non-neglecting, especially at the regional scale. In this paper, we focus on the short-term phenomena of hydrology. Therefore, in this study, we considered precipitation as the focused climate variable in further applications. It is essential to have reliable precipitation outputs from GCMs, which should reflect the current climate and represent zonal monsoon variabilities, such as the northeast and southwest monsoons and meridian wind, to address the implications of climate change. However, different GCMs produce varied climatic outputs owing to parameterisation and boundary conditions (Walker et al., 2003). As a result, their performance varies, and Koike et al. (2015) and Nyunt et al. (2016) developed a method for selecting GCMs based on their performance across a specific region by evaluating their major meteorological aspects in order to reduce the uncertainty of regional estimates made by GCMs. This approach chooses GCMs that can describe regional climate characteristics by comparing the model outputs with various data sets. The study considered precipitation, air temperature, outgoing longwave radiation, geopotential height, specified humidity, zonal wind, meridional wind, sea surface temperature, and sea level pressure. The downscaling method is critical because it affects the uncertainty of regional climate produced by GCMs (Zhang et al., 2020). Both statistical and dynamic downscaling methods have advantages and limitations regarding downscaling the GCMs' climatic variables for the regional scale (Zhang et al., 2020). Nyunt et al. (2016) developed a statistical bias correction approach that consists of three steps. The goal of this method is to minimise the amount of bias originating from GCMs by considering extreme precipitation, the number of wet days and dry days, and normal monthly precipitation biases (Nyunt et al., 2016). The Data Integration and Analysis System (DIAS) is a web portal platform that offers numerous services, one of which is the projection of multiple climatic variables of GCMs (Koike et al., 2015; Selvarajah et al., 2021). This system employs the three-step bias correction method and statistical downscaling functions developed by Nyunt et al. (2016) (Kawasaki et al., 2017). Climate sensitivity is crucial in decision-making, and this sensitivity is associated with a wide range of uncertainty related to the structure of GCMs, as Mauritzen et al. (2017) investigated (Mauritzen et al., 2017; Räihä, 2019). Some GCMs indicate significant discrepancies in climate projections, while others show minimal changes (Räihä, 2019). Working group I of the IPCC employs two standard techniques to describe the degree of certainty associated with significant findings: (1) based on the type, quantity, quality, and consistency of evidence, confidence is a qualitative assessment of the validity of discovery and degree of agreement, and (2) the likelihood technique provides a probabilistic expression of the amount of uncertainty in findings (IPCC, 2014). Because of the internal architecture, some GCMs produce contradictory results of the temporal variability among future climate projections. The causes behind the contradictory results of these GCMs should be presented in order to have a better understanding of decision-making.

This study focuses primarily on the effects of climate change on precipitation, taking into account the regional spatial and temporal variabilities to convey scientific findings for establishing a decision-making support system based on the five principles by addressing models, climate zones, and temporal change uncertainty. Accordingly, this study aims to resolve the uncertainties mentioned above by incorporating relevant accomplishments and developing a thorough approach to using GCMs for decision-making on regional and local scales. This analysis considered observed regional climate data and projected data from various GCMs under the Representative Concentration Pathway (RCP) 8.5. This research paper is structured in the following manner: Section 1 comprises the overall research framework, introduction, and problem statement. Section 2 elaborates on the study area and its features. Section 3 details the data and methodology for selecting GCM models and statistical bias correction and downscaling for GCM rainfall. It also provides an analysis of present and future seasonal rainfall data and projections and a methodology for addressing regional uncertainty in decision-making. Section 4 presents data analysis and simulation with discussions and information for decision-making. Section 5 concludes with a summarized conclusion and recommendations for future research endeavours.

1.2. Research framework

This research focuses on developing a research framework to address the spatial, temporal, and regional uncertainties present in future climate projections and to support sound decision-making. We introduced five principles for employing GCMs in decision-making in this new research framework. In addition, this study examines the expected climate change signals and investigates the factors contributing to the uncertainty of GCMs. Here, it is proposed to present a new color-coded climate change matrix, also known as the C4-Matrix, which can be used for decision-making on regional and local scales. The conceptual outline of this research for this particular study is presented in Fig. 1. There are three primary elements to form the research framework: (1) scientific approach, (2) analyses of the effects of climate change on seasonal events (seasonal precipitation changes spatially, temporary), and (3) the simplification of the procedures involved in decision-making in order to address the socio-economic approach. In Section 3, the particulars of the three primary components are described.

2. Study area

To address the five principles embedded in the new decision-making framework, choosing a diversified region with various spatial and temporal climatic zones, geography, landscape, and socioeconomic conditions is critical. We chose Sri Lanka because it has a diverse geography and tropical climate with two monsoon systems, and we can examine the distinct variabilities of the dry and wet seasons. Furthermore, different parts of the country (North, East, South, West, and Central) represent different climatic zones, such as arid, dry, intermediate, and wet. It features clearly-defined climatic zones and a wide range of diversity (Fig. 2, Fig. 3, and Fig. 4).

Sri Lanka is an island off the south-eastern coast of India with a land size of approximately 65,610 km^2 and a coastline of 1340 km (USAID, 2015). It is home to approximately 22 million inhabitants (Central Bank of Sri Lanka, 2020). Sri Lanka is sensitive to climatological influences from the Indian Ocean and the Indian subcontinent due to its geographical location (Ranasinghe, 2010), and the country was ranked second in the 2017 Climate Risk Index because of its high vulnerability to floods, droughts, and landslides (Eckstein et al., 2019). The country's landscape includes high central hills, flat plains, and coastal plains (Fig. 3). The country is one of the warmest in the globe, with average annual temperatures varying from 26.0 °C to 28.0 °C along the flat and coastal plains and 15 °C to 19 °C above 1500 m at higher-elevation regions (USAID, 2015). Sri Lanka receives approximately 1850 mm (ranging from 900 mm to 5000 mm) of average annual precipitation from three main sources: monsoon, convection, and depression

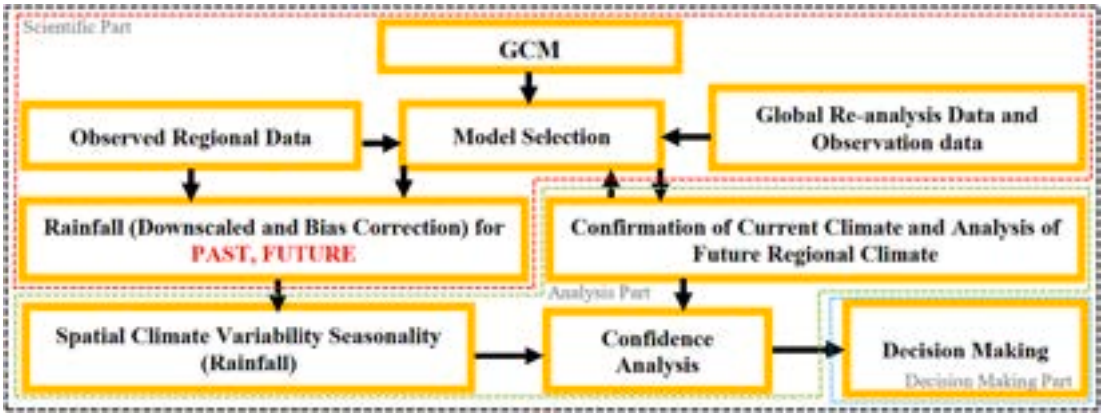

Fig. 1. Overall research framework.

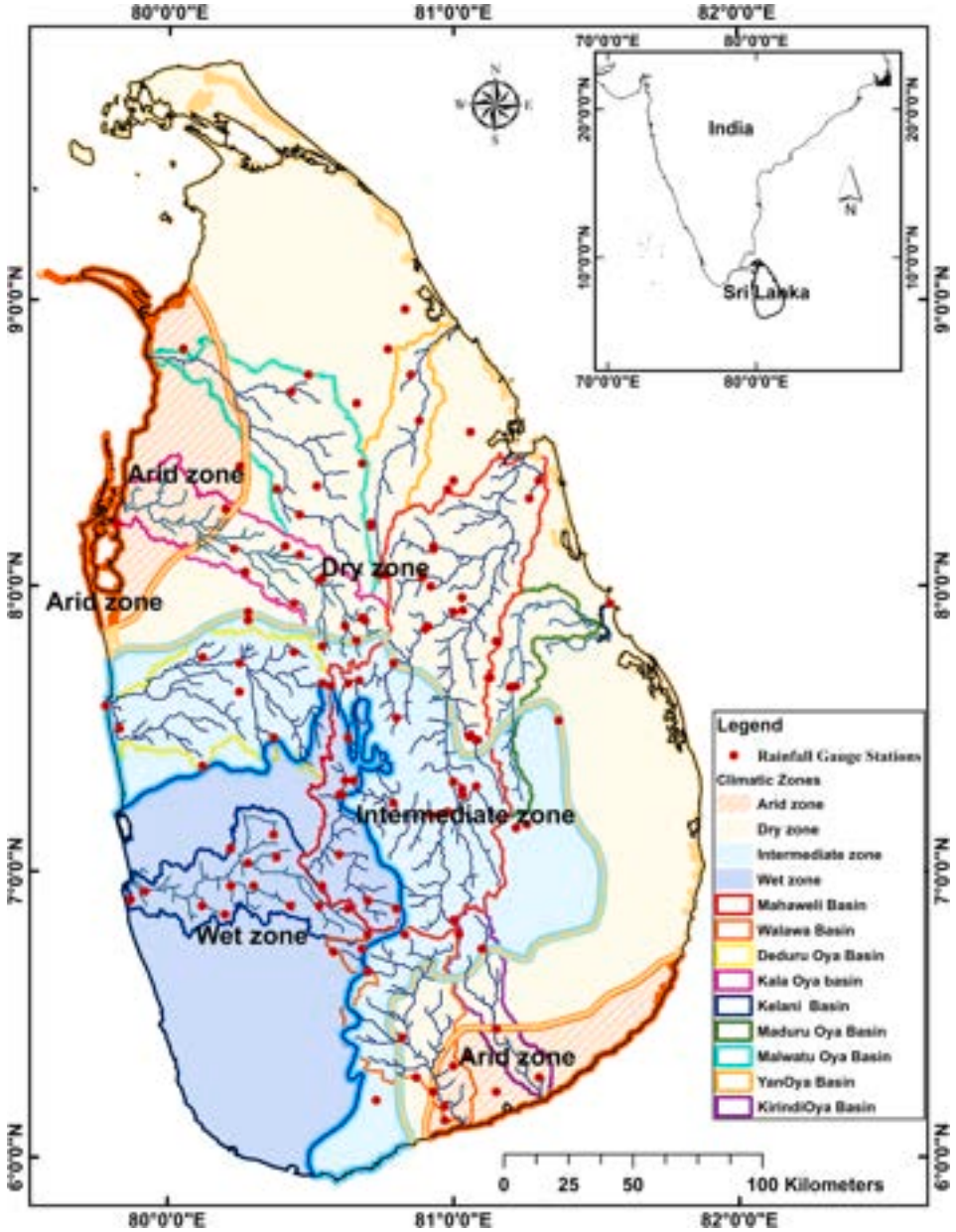

Fig. 2. Study area with climatic zones.

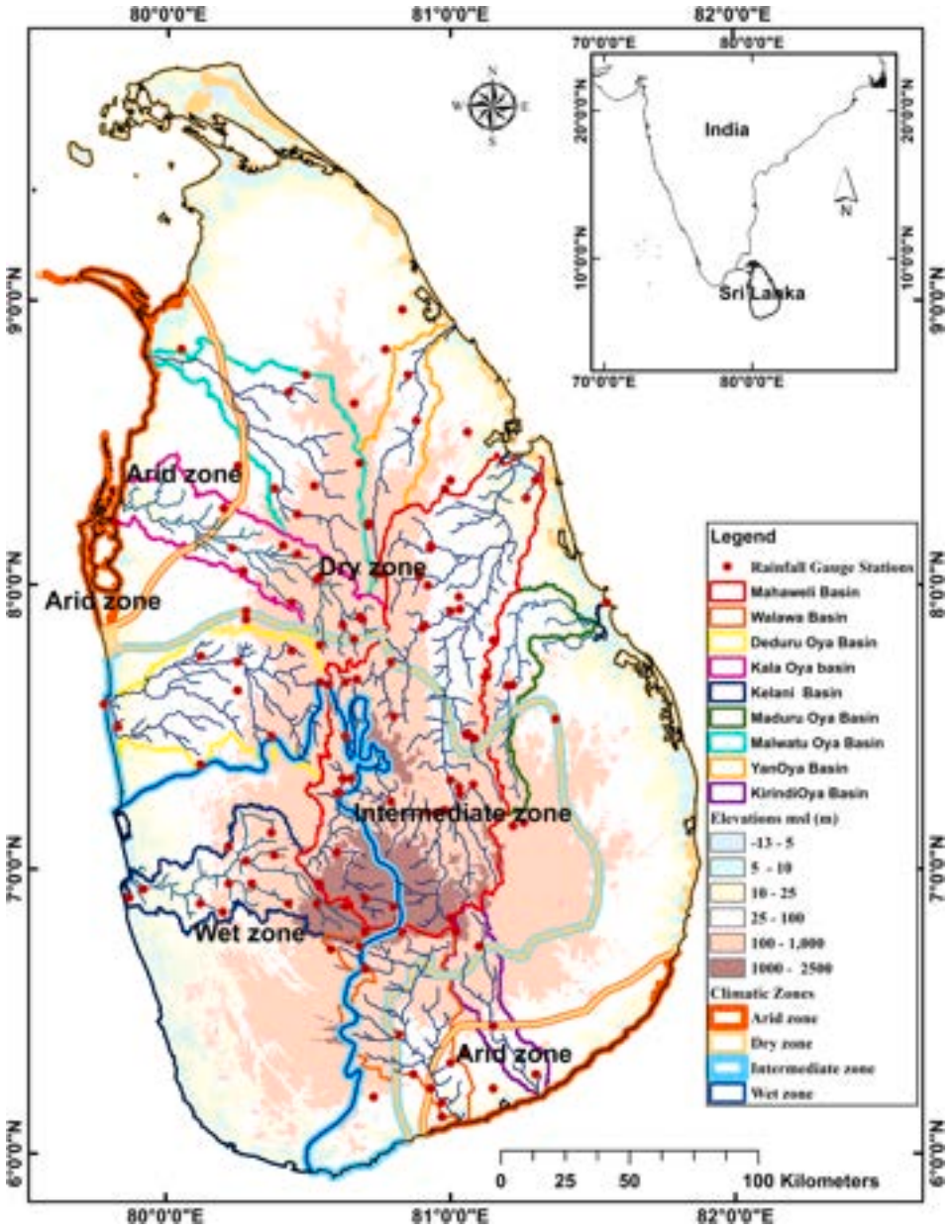

Fig. 3. Distribution of topography and climatic zones in the study area.

(Ministry of Mahaweli Development and Environment, 2016). Monsoon precipitation is influenced primarily by variations in heat and pressure over the Tibetan plateau, the Siberian plateau, the south Indian Ocean, the subtropical jet stream, the tropical easterly jet, the inter-tropical convergence zone (ITCZ), the Somali jet, the Somali current, the Indian Ocean Dipole (IOD), and the Indian Ocean branch of the walker cell (IAS, 2016; Saroha, 2017). Based on the precipitation-receiving mechanism, Sri Lanka has four monsoon seasons. Inter-monsoon 1 (IM-1) occurs from March to April and contributes to around 14 % of the country's annual mean precipitation, whereas the Southwest monsoon season (SWM) occurs from May to September and accounts for about 30 % of the annual mean precipitation. Inter-monsoon 2 (IM-2) typically occurs from October to November, providing up to 30 % of the annual mean precipitation in just two months, while the North East monsoon season (NEM) occurs from December to February, bringing 26 % of the mean annual precipitation (Ministry of Mahaweli Development and Environment, 2016). Two arid zones, found in the northwest and southeast, receive meagre precipitation, with mean annual precipitation ranging from 800 mm to 1200 mm, while dry zones, found in the north and east, receive mean annual precipitation ranging from 1200 mm to 1750 mm predominantly from the northeast monsoon (Fig. 2 and Fig. 3). The majority of the intermediate zones (Fig. 3) in the central and eastern areas receive rainfall between 1,750 mm and 2,500 mm per year, primarily from the northeast monsoon, whereas the wet zone (Fig. 3) in the south-western slopes of the central hills receives the heaviest precipitation of more than 2,500 mm per year, mainly from the southwest monsoon (WB and ADB, 2020).

There are 103 river basins in Sri Lanka, most of which originate in the central highland mountains (Fig. 3) and flow approximately 33 billion cubic meters into the Indian Ocean (WB and ADB, 2021). This study investigates nine major river basins in Sri Lanka: Walawa, Kelani, DeduruOya, KalaOya, MalwatuOya, YanOya, Mahaweli, MaduruOya, and KirindiOya, covering all four climatic zones (Fig. 2). All selected basins are adjacent to the Mahaweli basin, and a few have *trans*-basin diversion water from it. Selected basins feature various types of landscape, such as urbanized, agricultural, and industrial areas, forests, and

Fig. 4. Natural forest diversity in the study area.

wilderness (Fig. 4). These landscape types are diversely spatially distributed in the basins. For example, the lower Kelani basin is heavily urbanized, whereas the lower MalwatuOya basin is covered with natural forests (Fig. 4). The country's most dense municipalities, including the capital, Colombo, Kandy, and Kurunegala, are located in study areas. These selected basins contribute more than two-thirds of the country's primary agricultural industry. In the study area, several tank/reservoir cascade systems exist, and medium and large reservoirs have been built across the represented rivers of the relevant basins for multiple purposes, such as irrigation, flood management, drinking water, and hydropower generation (Arumugam, 1969). The main hydropower plant complexes, such as Mahaweli, Kelani, and Walawa hydropower complexes, are located in the study area and provide more than half of the country's total electricity demand (total installed main hydropower capacity: 1470 MW), and some of the main thermal power plants are located in the Kelani basin. The Mahaweli River basin is the largest in Sri Lanka, which covers about one-fifth of the country, flowing across the major climate zones. Due to its flow direction, the Mahaweli basin neighbours the country's main river basins, sharing most of its water resources. The Mahaweli Authority regulates the Mahaweli water because the basin has the most extensive variability of water resources and the widest variety of statistically temporal resources in the nation. As a result, the study area significantly impacts the socioeconomic conditions of the country. For our research, we decided to focus on the Mahaweli basin and its main neighbouring basins because they include a significant impact and connection of climatological, geographical, sociological, and economic variety. Table 1 and Fig. 2 provide the salient details (The national atlas of Sri Lanka, 2012) of the target basins and a detailed figure of the study area. In this manuscript, we are exclusively concerned with precipitation as a climatic variable and its statistics such as mean precipitation, cumulative precipitation, seasonal variability, and inter-annual variability.

3. Methods and materials

3.1. Methodology

The methodology for our investigation is described in detail in the

Table 1
Details of the Target basins.

No	Name of Target Basins	Catchment Area (km^2)	Climatic Zones	Annual Average Discharge to Sea (MCM)	Elevation variations (m)
1	Kelani	2278	W	3417	−1.8–2300
2	DeduruOya	2616	IM, W	1608	0–1050
3	KalaOya	2772	IM, D, A	386	0–870
4	MalwatuOya	3246	D, A	192	0–725
5	YanOya	1520	D, A	132	0–450
6	MaduruOya	1541	IM	226	0–510
7	Walawa	2442	W, IM, D, A	350	0–2300
8	KirindiOya	1165	IM, D, A	74	0–1550
9	Mahaweli	10,327	W, IM, D	4009	0–2550

Note: W (WET), IM (Inter-Mediate), D (Dry), A (Arid) climatic zones.
Source: National Atlas published by the Survey Department in 2012.

following paragraphs. This section is organized into the techniques, GCM selection, input data, and model setup used in the five principles to investigate uncertainty in climate projections. Supplementary Table A.3 summarizes additional information concerning data collecting, processing, and analysis methodologies relevant to our research.

3.1.1. Introduction of DIAS system

The Data Integration and Analysis System (DIAS) is a centralized platform developed and operated by the University of Tokyo, funded by the Ministry of Education, Culture, Sports, Science and Technology (MEXT) in Japan. It provides access to earth observation data and facilitates processing, assimilation, and interpretation of the data. DIAS system processes data collections and integration platforms that collect and combines data from satellites, ground observation (e.g., rainfall), weather prediction models, and climate change projection from GCMs (i.e., GCMs of Coupled Model Inter-comparison Project Phase 5). This system has over 25 PB of data storage and analytical space and cluster servers for analysis, producing over 2000-core processing power. It delivers a comprehensive collection of various Earth observation data to researchers and user-friendly tools for data discovery and retrieval. Researchers can extract useful insights from satellite imagery and perform tasks like image processing and change detection through the system's superior processing and analysis capabilities. It is a vital resource for disaster management, environmental monitoring, urban planning studies, agriculture, biodiversity, health, and energy studies, contributing to scientific developments and evidence-based decision-making not only in Japan but also in the global Earth observation community (Kawasaki et al., 2018). The system provides visualization tools, format exchange tools, correlation analysis tools, data-seeking help tools, and a bias correction and downscale tool for climate data. More information on the DIAS system can be found in Kawasaki et al. (2018).

This study utilized DIAS's CMIP5 data platform and climate variables analysis tools. We analysed JRA-55 and other reanalysis data with CMIP5 data to evaluate climate model replication using the system tool and functions. Using bias correction and downscaling tools, we corrected bias between GCMs and observation precipitation data. The visualization tool was used to do a difference analysis of average seasonal and annual climatic variables. The research should comprehensively examine all climate model results. As a result, all model outputs should be archived or examined in the same way. Except for the DIAS web portal platform, this type of analytical option is not available and has not been provided. CMIP6 analysis environment has not yet been implemented by DIAS. CMIP5 is used for this research due to the DIAS's current capabilities and more consistent comparisons and interpretations of results from previous studies.

3.1.2. GCM selection

GCM projections have a high degree of uncertainty, as mentioned in Section 1.1; hence, it is critical to choose models that can represent the past and current climatology in a specific climatic region (Nyunt et al., 2016; Selvarajah et al., 2021). We employed a thorough strategy to discover best-performing GCMs for basin-scale climatology analysis. This strategy employs observed, global, and GCM climate data that are relevant to regional precipitation mechanisms (Nyunt et al., 2016; Selvarajah et al., 2021). Projection of precipitation based entirely on observed or reanalysis precipitation is insufficient since other climatological variables (e.g., sea surface temperature, zonal wind, meridional wind, and sea surface pressure) interact with the mechanism of precipitation in the climate system. Therefore, various climatological characteristics are also important in determining best-performing GCMs (multi-model selection). This study assessed and evaluated eight global and regional climatological variables, including precipitation (Pr), air temperature (T_{air}), outgoing longwave radiation (OLR), zonal wind (ZW), meridional wind (MW), sea level pressure (SLP), sea surface temperature (SST), and geopotential height (GPH), to identify best-performing GCMs for regional precipitation. Finally, the multi-model selection was made by comparing GCM performance with the observation and reanalysis of the above-climatological variables for the historical period (1980–2005) for interested regional and local domains. These climatological variables have diverse influencing and processing domains, and it is critical to capture the relevant influencing domain that represents the synoptic scale of the relevant phenomena of the precipitation mechanism. Therefore, different domain scales for the relevant specified variable that represent the key synoptic-scale phenomena are chosen, and the performance of selected GCMs is quantitatively compared for GCM past climate simulation outputs using spatial correlation indices (Scorr) and root mean square error indices (RMSE) (Nyunt et al., 2016; Selvarajah et al., 2021).

$$Scorr = \frac{\sum_{i=1}^{N}(x_i - \bar{x})(y_i - \bar{y})}{\sqrt{\sum_{i=1}^{N}(x_i - \bar{x})^2 (y_i - \bar{y})^2}} \tag{1}$$

$$RMSE = \sqrt{\frac{1}{N}\sum_{i=1}^{N}(R_{si} - R_{obs})^2} \tag{2}$$

where x_i is the values of the GCM's variable in a given period, $\bar{x}$ is the mean of the values of the GCM's variable in a given period, and y_i is the mean of the values of the reference (observed/re-analysis) source variable in a sample, while $\bar{y}$ is the mean of them. R_{si} is the value of the relevant climate variable of the GCM, R_{obs} is the value of the relevant climate variable of the reference (observed/re-analysis) source, and N is the total number of months.

The past regional or local monthly average rainfall is computed to determine the variance in rainfall and to identify the annual past climate seasonal variable signal. The DIAS archives 61 GCM model outputs from CMIP5. The DIAS web portal, which is an embedded tool for simulating and comparing GCM outputs with historical reference-related climatology data over the study area, is used to calculate the monthly, seasonal, and annual Scorr and RMSE of each selected climatological variable of GCMs compared to observations or reanalysis data (Kawasaki et al., 2017). After that, the average seasonal and annual Scorr and RMSE of each climatological variable (8 climatological variables) were computed for the ensemble of all GCMs. For each GCM, skill scores (0 and 1) for two indices were introduced based on the individual performance of the GCMs and the average performance of the ensemble of all GCMs.

The model was assigned using the following scoring criteria:

$$Index_{scorr} = \begin{cases} 1, & if\ Scorr_{model} \geq Scorr_{total\ average} \\ 0, & otherwise \end{cases} \tag{3}$$

$$Index_{RMSE} = \begin{cases} 1, & if\ RMSE_{model} \le RMSE_{total\ average} \\ 0, & otherwise \end{cases} \quad (4)$$

$$Index_{total} = \begin{cases} 1, & if\ Index_{scorr} = 1\ and\ Index_{RMSE} = 1 \\ 0, & if\ Index_{scorr} = 1\ and\ Index_{RMSE} = 0\ or \\ & if\ Index_{scorr} = 0\ and\ Index_{RMSE} = 1 \\ -1, & if\ Index_{scorr} = 0\ and\ Index_{RMSE} = 0 \end{cases} \quad (5)$$

Where, $Scorr_{model}$ is the spatial correlation score of the model, $Scorr_{total\ average}$ is the total average spatial correlation score, $RMSE_{model}$ is the Root Mean Square Error score of the model, $RMSE_{total\ average}$ is the total average RMSE score, and $Index_{total}$ is the total index.

The total index for each model's associated meteorological variables is computed, and then the total indexes for each model's associated meteorological variables are summed to get the total. This methodology is employed to sum up all grand total indexes (seasons and annuals) for designated seasons that correlate to the local study region of interest. Then, all GCMs were ranked based on the grand total value. As precipitation is the key factor, only high-ranking GCMs with a positive total index for the precipitation variable were considered for the final selection. Finally, odd numbers ($> = 3$) of GCMs were chosen for the investigation to provide a better confidence explanation.

3.1.3. Statistical bias correction and downscaling precipitation

By considering GCMs' uncertainty, we first choose GCMs that can reproduce the current climate of the study area. Because GCMs are incapable of directly resolving features of regional climate variability due to coarse resolution and model uncertainty, downscaling from global to regional scale is required (Moise et al., 2015). High spatial distribution of precipitation stations leads to less uncertainty in precipitation-relevant simulation, and thus a high spatial precipitation network in the target basin leads to a less uncertain regional climate model (Moreira et al., 2006; Smitha et al., 2018). Therefore, this research utilized data from a dense network of 120 rain gauge stations for the targeted basins. As our research aims to address the model uncertainty of multiple GCMs across different time scales (near future, middle future, and far future), it necessitates significant computational and analytical requirements. As a result, dynamic downscaling is more expensive, necessitating substantial technical resources and time. On the other hand, statistical downscaling offers a faster and less resource-intensive alternative that is adaptable to various geographies and variables. It allows for long-term climate analysis and can handle non-stationarity in climate patterns. Therefore, for this study, a more feasible approach is necessary to tackle the model uncertainty of multiple GCMs. Hence, the statistical downscaling method is selected as a feasible option. Gridded precipitation data from GCMs were downscaled to 120 observation stations (points) using the inverse distance weighted (IDW) approach (Kawasaki et al., 2017). Subsequently, the biases between the GCMs' and observed data were corrected using the three-step statistical bias-correction methodology (Nyunt et al., 2016) through the DIAS-CMIP5 web portal tool. This three-step bias correction method uses the Generalized Pareto Distribution, the Gamma distribution, and the Statistical Ranking Order to minimize bias in extreme precipitation, regular monthly precipitation, and no precipitation days, respectively (Nyunt et al., 2016). The method of moments (MOM) was utilized to estimate the parameters of the GPD in this case, and seasonal extreme bias correction was also performed. Finally, to correct for bias in the GCM simulations, the GPD is fitted to the extreme rainfall data (Nyunt et al., 2016). The same transfer functions at the respective stations were used to bias-correct the projected future precipitation. The Thiessen polygon average was taken to represent the average GCM precipitation for each basin by considering each station's bias-corrected GCM precipitation.

3.1.4. Sensitivity analysis

In this study, we investigate the sensitivity of GCMs by evaluating the degree of variation in average precipitation temporally and spatially. GCMs are categorized into high, medium, or low sensitivities based on the difference between past (1980–2005) and future (26-year span: 2025–2050, 2050–2075, and 2075–2100) average annual precipitation over a basin. If the degree of difference is less than 25 %, they are considered low-sensitivity GCMs; if between 25 and 50 % or greater than 50 %, medium- or high-sensitivity GCMs, respectively.

$$DOD = \{(P_f - P_p)|P_p\}*100\% \quad (6)$$

Where DOD is the degree of a difference, P_f refers to future average seasonal or annual precipitation, and P_p refers to past average seasonal or annual precipitation.

Future precipitation patterns were classified as an increasing trend (DOD $>$ 0) or decreasing trend (DOD $<$ 0) over a certain spatial and temporal range for each GCM's outputs. The number of GCMs with a positive and negative trend for DOD is counted separately. Based on the type of trend, the confidence level for future decision-making is introduced, which is comparable to the method used in IPCC-AR5: 0–5% extremely unlikely, 0 $<$ 50 % more unlikely than likely, $>$50–100 % more likely than not, and 95–100 % extremely likely (IPCC, 2014). Our study considered the following qualitative levels of confidence: extremely unlikely (if all five models disagree), more unlikely than likely (if one or two models agree), more likely than not (if three or four models agree), and extremely likely (if all five models agree). We used only two high confidence levels, more likely than not and extremely likely, to reflect three or more models with the relevant agreement in the case of five selected GCMs (3/5–5/5). Furthermore, the linear trend was employed to evaluate the variability of observed seasonal and annual precipitation in the past, which represents the ongoing rise or fall over time.

3.1.5. Identification of discrepancies in outcomes among climate models

Differences in outcomes amongst climate models were investigated in order to determine the cause of contradictory precipitation mechanisms through the DIAS web system. Regional monsoon periods (NEM, SWM) were set up, and the optimal behaviour of eight climatological variables (air temperature, outgoing longwave radiation, sea level pressure, zonal wind, geopotential height, sea surface temperature, wind vector, and meridional wind) in the current and future climates was investigated.

3.2. Data

For this study, we used a variety of spatial and temporal observed precipitation data, reanalysis climatological data, remote sensing data, and GCM data.

3.2.1. Observed data for GCM selection and bias correction

We utilized observed daily precipitation data from 122 meteorological stations in nine basins from 1980 to 2015 (Fig. 2), which were obtained from respective Sri Lankan organizations (viz., Irrigation Department, Department of Meteorology, Mahaweli Authority of Sri Lanka, Mahaweli Water Security Investment Program). The spatial details of the rain gauge stations and their corresponding climatic zone and annual average precipitation are listed in supplementary material Table A.1. Consistency checks were performed for observation data by comparing them with the precipitation data from nearby weather stations. The Inverse Distance Weight (IDW) method was used to fill in some missing data for a few meteorological stations (Shepard, 1968). We analyzed observed precipitation data from all 122 stations for the study in order to identify the precipitation signals (durations) of past basin precipitation (Fig. 6). The Thiessen polygon method, initially proposed by Thiessen et al. (1911) and commonly recommended for

meteorological assessment (Das, 2018), was utilized to analyze the average precipitation of the basin. We utilized the observed precipitation data from 120 stations (points) to downscale (grid data to point data) and bias-correct the GCM precipitation data for each station. We employed a statistical downscaling approach using the inverse distance weighted (IDW) method (Kawasaki et al., 2017) and a three-step bias correction method (Nyunt et al., 2016) to correct the bias in GCM data at the observation stations (points). Furthermore, high-density rainfall station networks for each basin were used to reduce the relevant average basin precipitation bias.

3.2.2. Data for GCM selection

To select best-performing GCMs for local-scale projections, we used historical reference climatological data, such as precipitation (Pr), air temperature (Tair), outgoing longwave radiation (OLR), zonal wind (ZW), meridional wind (MW), sea level pressure (SLP), sea surface temperature (SST), and geopotential height (GPH), from 1980 to 2005. These data were collected from institutions worldwide and embedded in the DIAS. The DIAS archives 61 GCM outputs from each Numerical weather prediction centre. However, some of these outputs do not include the required time period and meteorological elements. As a result, 44 GCMs are used for the target of model selection, excluding 17 GCMs in advance to address the uncertainty of model selection. By choosing a large number of GCMs with different modelling methodologies, sets of parameters, and structural arrangements, we can identify the best regional climate-capturing GCMs. The inclusion of a larger number of GCMs allows us to identify those that have shown good results in simulating historical climate conditions and reproducing observed climate patterns. Pr and OLR at the top of the atmosphere, and SST data were obtained from the Global Precipitation Climatology Project (GPCP) dataset (Adler et al., 2003), the National Oceanic and Atmospheric Administration (NOAA) (Liebmann and Smith, 1996), and the Hadley Centre (Rayner et al., 2003), respectively. The remaining daily variables, such as T_{air}, ZW, MW, and GPH, were obtained from the Japanese 55-year Reanalysis (JRA-55) (Kobayashi et al., 2015). Monthly data (historical reference data) from GPCP, NOAA, Hadley Center, and JRA-55 are used for the calculation of S_corr and RMSE between CMIP5.

Because different climate drivers have varying influences in different domains, three spatial domains were explored across the study area to evaluate the performance of GCMs on regional and local scales. This was done to account for the effects of key main climatic drivers, such as Asian monsoons, the Indian Ocean Dipole (IOD), the intertropical convergence zone (ITCZ), and the El Niño-Southern Oscillation (ENSO), on events that influence the climate patterns of the research region (Annamalai et al., 2004; Sahu et al., 2010). We assessed eight climatic variables in this study, and Table 2 indicates the domains that were chosen for key climatic variables. Fig. 5 displays the small, large, and very large domains utilized for assessing climatological variables in order to select the best GCMs for regional usage. Furthermore, the SWM and NEM monsoon seasons were defined basin-wise based on the period of average observed southwest and northeast monsoonal precipitation in the basins to describe its temporal and seasonal climatological variabilities, and precipitation (Pr) was considered as a key climatological parameter in the final selection of GCMs that represent good agreement with the current climate.

3.2.3. Past and future GCM climate data

Historical reference climatological data from different institutions across the world were used in this study from 1980 to 2005. Climate projections from the four scenarios, i.e., RCP2.6, RCP4.5, RCP6.0, and RCP8.5, defined and endorsed in the IPCC fifth assessment report (AR5), are available from the Coupled Model Inter-comparison Project Phase 5 (CMIP5) model outputs of several experiments (IPCC, 2013). All projected data are available in the DIAS system. In this study, we examined CMIP5 outputs relevant to RCP8.5 (i.e., business-as-usual scenario) from the DIAS system for historical and future projection data. Our choice of RCP 8.5 was driven by our objective to project the potential consequences under extreme conditions. By examining this scenario, characterized by significant greenhouse gas emissions, we could gain insights into the effects of the most extreme climate change scenario. RCP 8.5 serves as an important tool to understand the upper limits of climatic scenarios, highlighting their associated hazards and vulnerabilities. Future precipitation projections were generated for three different periods: the near future (2025–2050), the middle future (2050–2075), and the far future (2075–2100).

Table 2
Domains for key climatic variables.

No	Climatic variable	Domain	Scale
1	Precipitation (Pr)	10^0N – 6^0S, 79^0W – 82^0E	Small
2	Air Temperature (T_{air})	20^0N – 15^0S, 45^0W – 110^0E	Large
3	Outgoing Longwave Radiation (OLR)	20^0N – 15^0S, 45^0W – 110^0E	Large
4	Sea Level Pressure (SLP)	20^0N – 15^0S, 45^0W – 110^0E	Large
5	Zonal Wind (ZW)	20^0N – 15^0S, 45^0W – 110^0E	Large
6	Meridional Wind (MW)	20^0N – 15^0S, 45^0W – 110^0E	Large
7	Geopotential Height (GPH)	20^0N – 15^0S, 45^0W – 110^0E	Large
8	Sea Surface Temperature (SST)	25^0N – 35^0S, 40^0W – 220^0E	Very Large

4. Results and discussions

Forty-four GCM model outputs archived in the DIAS system were evaluated using the technique described in Section 3 for selecting five best-performing GCMs for local or regional applications. The precipitation from best-performing GCMs was used after statistically downscaling and bias-correcting GCM outputs by considering observed precipitation. Four sets of GCM outputs (i.e., past and three periods of future climate) and a set of observed data were analyzed in this study. The past climate analysis was conducted for 26 years during the historical observed and model-simulation period (1980 to 2005), whereas the future climate analysis was conducted using the RCP8.5 scenario for the same 26-year period as the near future (NF), the middle future (MF), and the far future (FF) from 2025 to 2050, 2050 to 2075, and 2075 to 2100, respectively. The sensitivity of the GCMs and the explanations for the diverse results are examined in the following sections. The likelihood agreement of the GCMs was used to project future trends. In this section, we mainly presented and discussed the results of climate change effects on precipitation and climate change signals while accounting for regional spatial and temporal variability in order to convey cutting-edge scientific findings for establishing a decision-making support system based on five principles while addressing model, climate zone, and temporal change uncertainty.

4.1. GCMs selection

Seasonal patterns are chosen for the local basin based on the observed average monthly precipitation of the basin, as indicated in Section 3.1.1. Basin average monthly observed precipitation (1980–2005) for selected diverse basins is shown in Table 3 and Fig. 6. Fig. 6 depicts two climate signals of most basins from February to July and August to January. Furthermore, as shown in Fig. 6, localized basins receive precipitation from both the Southwest monsoon (SWM) and the Northeast monsoon (NEM), with the NEM providing significantly more monthly precipitation for all basins most of the time. Based on the scoring technique described in Section 3.1.1, five high-performing GCMs were chosen for further analysis of the basin variability of projected precipitation. As an example, the best performance of the GCMs for the

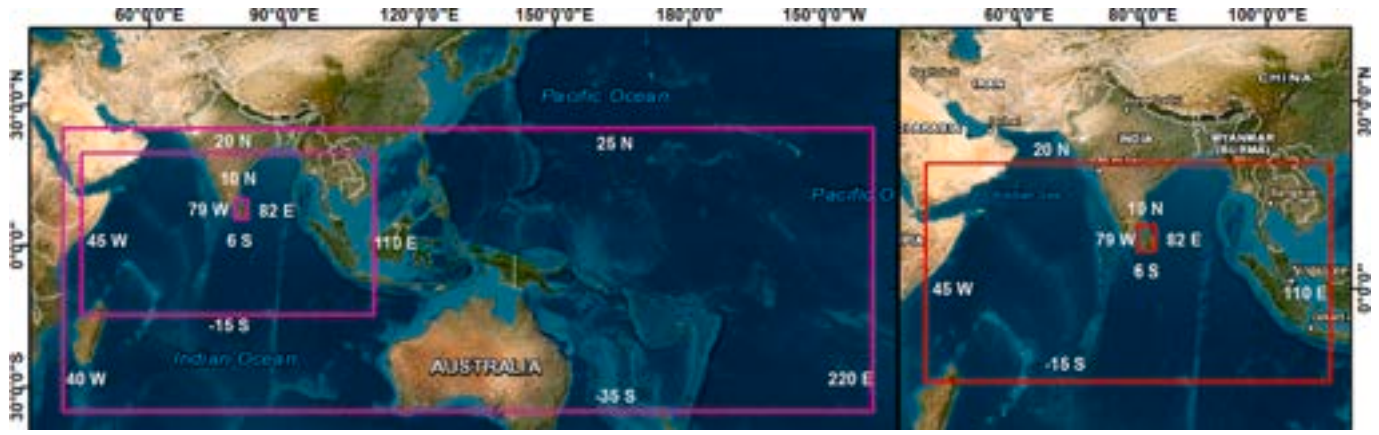

Fig. 5. Small, large, and very large domains for evaluating the GCMs' climatological parameters.

Table 3
Average annual observed precipitation for the 26 years (1980–2005).

Months	Basins Average Annual Precipitation (mm/year)								
	Walawa	Kelani	Deduru-Oya	KalaOya	MalwatuOya	YanOya	Mahaweli	Maduru-Oya	Kirindi-Oya
January	103	111	76	86	81	114	213	247	84
February	91	98	57	64	54	60	114	117	75
March	146	168	83	55	47	38	84	65	115
April	229	344	208	162	122	93	132	111	169
May	143	411	136	81	65	49	107	69	98
June	76	395	88	21	15	11	84	14	25
July	54	309	58	25	30	42	95	39	34
August	55	249	46	19	28	39	83	47	32
September	103	351	115	68	72	96	128	92	83
October	219	456	283	208	187	168	223	196	204
November	292	392	276	241	232	246	301	288	278
December	162	170	118	161	182	222	300	332	150

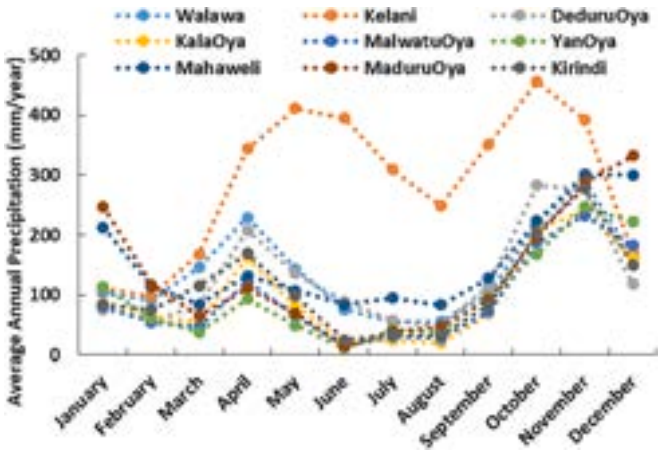

Fig. 6. Basin average annual precipitation for the 9 basins.

Walawa basin is shown in Table 4. For the Walawa basin localized region, best-performing GCMs were chosen according to the highest grand total and excluding seasons with poor precipitation signals. Table A.2 (attached as supplementary material) summarizes the GCMs' performance for the Walawa basin. Because the Maha season is crucial for the Sri Lankan domain, the precipitation index for the Maha season was examined. However, GCMs with a negative precipitation index were not chosen. Moreover, models that did not provide projected future precipitation for the relevant RCP8.5 were eliminated from the final model selection. After evaluating those criteria for respective GCMs, the final five GCMs, i.e., ACCESS1.0, CNRM-CM5, CanESM2, IPSL-CM5A-MR, and MIROC5, were chosen for the Walawa basin for further precipitation analysis, such as downscaling and bias correction.

The same methodology was used to identify best-performing GCMs for other diverse eight basins and local regions. To select best-performing GCMs for the Mahaweli basin, 20 years of precipitation were analyzed and compared with the findings of Selvarajah et al. (2021). Table 5 summarizes the best-performing GCMs selected for the localized diverse basins (regions).

According to Table 5, the same five GCMs perform well for the Walawa, DeduruOya, Kelani, and KirindiOya basins, which belong to the climate zones that are either entirely or partially in one or both Intermediate, wet zones and face the SWM direction. Another group of the same five GCMs performs well in the MalwatuOya, KalaOya, and MaduruOya basins, which belong to the climate zones that are entirely or partially in the dry zone and face the NEM direction. The YanOya basin is the narrowest basin facing the NEM direction and the only basin entirely within the dry zone. The same four GCMs also perform well in this YanOya basin. The resolutions of the selected GCMs for these local basins vary, and some selected GCMs have highly coarse resolutions (CanESM2, IPSL-CM5A-MR, and GFDL-ESM2G). The latitudinal and longitudinal grid sizes of the selected GCMs are ACCESS 1.0 (1.25^0, 1.88^0), ACCESS 1.3 (1.25^0, 1.88^0), CNRM-CM5 (1.40^0, 1.41^0), CanESM2 (2.79^0, 2.81^0), IPSL-CM5A-MR (1.27^0, 2.50^0), MIROC5 (1.400, 1.41^0), MPI-ESM-LR (1.86^0, 1.88^0), and GFDL-ESM2G (2.02^0, 2.00^0). Fig. A.1 (attached as supplementary material) illustrates the locations of the grids for each selected GCM. According to Table 5 and Fig. A.1, coarse-resolution GCMs perform well in our selection techniques (CanESM2, IPSL-CM5A-MR).

Table 4
The best performance of the GCMs for the Walawa basin. High-performed (Selected) GCM details were bold.

	Model Name	Institute	Country	Signal-1		Signal-2		Signal −3		Total Index Precipitation	Total grand Index	Ranked Selected Model	Remarks
				Yala Season		Maha Season		Annual-12 Months					
				Precipitation index	Total Index	Precipitation index	Total Index	Precipitation index	Total Index				
7	**CanESM2**	**CCCMA**	**Canada**	**1**	**7**	**1**	**4**	**1**	**5**	**1**	**16**	**1**	**Selected**
15	**CNRM-CM5**	**NCMR**	**France**	**1**	**5**	**1**	**6**	**1**	**5**	**1**	**16**	**2**	**Selected**
32	**IPSL-CM5A-MR**	**IPSL**	**France**	**1**	**5**	**1**	**4**	**1**	**4**	**1**	**13**	**3**	**Selected**
37	**MIROC5**	**UT**	**Japan**	**1**	**3**	**1**	**5**	**1**	**5**	**1**	**13**	**4**	**Selected**
1	**ACCESS1.0**	**CSIRO-BOM**	**Australia**	**0**	**6**	**1**	**7**	**1**	**7**	**0**	**20**	**5**	**Selected, SPP-M**
6	CanCM4	CCCMA	Canada	1	7	1	5	1	6	1	18		UFP
13	CMCC-CESM	CMCC	Italy	−1	4	1	7	1	7	0	18		VPPP
14	CMCC-CMS	CMCC	Italy	1	8	0	−1	0	6	0	13		VPPP & UTI
16	CNRM-CM5-2	NCMR	France	1	5	1	5	1	5	1	15		UFP
38	MPI-ESM-LR	MPI-N	Germany	1	8	0	5	1	8	0	21		PPP-M
39	MPI-ESM-MR	MPI-N	Germany	1	7	0	7	1	7	0	21		PPP-M
40	MPI-ESM-P	MPI-N	Germany	1	8	0	5	1	7	0	20		PPP-M

Note: PPPA = Poor Precipitation Performance Annual, PPP-M = Poor Precipitation Performance in Maha season, SPP-M = Satisfactory Precipitation Performance in Maha Season, UFP-Unavailability of Future Precipitation, VPPP = Very Poor Precipitation Performance, UTI = Unsatisfactory Total Index.

4.2. Seasonal and annual precipitation variability in the historical period

The average seasonal and annual precipitation is calculated using observed precipitation data from 122 stations between 1980 and 2005. Fig. 7 illustrates the average annual and seasonal precipitation for the entire basin. As indicated in Section 2, our selected diverse basins, and regions experience precipitation primarily during four seasons: IM-1, SWM, IM-2, and NEM. Two basins (KalaOya and MalwatuOya), whose lower portions are located in an arid climate zone, reflect an annual arid climate. However, YanOya, which is located exclusively in a dry zone, also displays an arid climate annually. The MaduruOya basin, which belongs to the dry and intermediate (IM) zones, had a dry climate annually in the past, whereas the DeduruOya basin, though belonging to the wet and IM zones, also had a dry climate annually in the past. The Kelani basin, which belongs to an entirely wet zone, exhibited a wet climate annually in the past; however, the Mahaweli basin, which belongs to the wet, IM, and dry zones, exhibited an IM climate annually in the past. The Walawa basin, which is the only basin belonging to all four climate zones, and KirindiOya, which partially belongs to the arid, dry, and IM climatic zones, exhibited a dry climate from 1980 to 2005. Furthermore, the basins have considerable variety in precipitation in different seasons (IM-1, SWM, IM-2, and NEM); for example, the Kelani basin had significant precipitation during SWM, whereas the northern and northwest (NW) basins received less precipitation than the Kelani basin. The Mahaweli basin, which neighbors all selected basins, experienced modest precipitation during SWM. Nonetheless, it received less precipitation throughout the IM-1 season compared to the other basins. During IM-2, all basins similarly experienced high precipitation variability, with the Kelani and DeduruOya basins receiving the highest precipitation. During NEM, the northern basins received high precipitation, with Mahaweli and MaduruOya receiving the most. Nonetheless, the Kelani basin received comparably less precipitation compared to the two seasons (SWM and IM-2). By investigating past basin-average annual precipitation, we discovered that the northern basins (YanOya, MalwatuOya, and KalaOya) had lower precipitation, which may cause metrological drought conditions in the basins.

4.3. Current climate analysis

4.3.1. Current climate of meridional wind (MW) and wind vector (WV)

As indicated in Section 3, we used the two optimal (clearly demonstrated behaviours) performed climatological variables, meridional wind (MW) and wind vector (WV), during the two main seasons to analyse the current climate (1980–2005). Figs. 8 and 9 depict the current climate for MW for the reference observed data (JRA-55) and the selected GCMs for two seasons: SWM and NEM. Fig. 8 shows that the meridional wind pattern and direction of all selected GCMs were confirmed from reanalysis data for SWM from 1980 to 2005 (current observed and reanalysis climate) under the Sri Lankan domain. The current version of DIAS CMIP5 analysis tool provides a color scale for representing the difference between future and past climatological variables. Nonetheless, the magnitude of the relevant reference reanalysis data and GCM data is fairly similar (0–4 m/s, south to north direction), and all GCMs produced the same pattern and direction in MW. Fig. 9 confirmed that the meridional wind pattern and direction of GCMs for NEM are consistent with the current climate. The magnitude of the relevant reference reanalysis data and GCM data is nearly the same (−6 – −2 m/s, north to south), and all GCMs produced the same pattern and direction in MW around our study area context. All the selected GCMs reasonably represent the current climate for the Sri Lankan domain in both seasons.

Figs. A.2 and A.3 (attached as supplementary materials) represent the current climate for WV for the reference observed data (JRA55) and the selected GCMs for SWM and NEM, respectively. Figs. A.2 and A.3 confirmed that the WV pattern and direction of GCMs for SWM and NEM are consistent with the current climate reference data (1980–2005). The

Table 5
Best-performing GCMs for the localized diverse basins.

No	Basin Name	Name of the General Circulation Model (GCM)							
		1	2	3	4	5	6	7	8
1	Walawa	ACCESS1.0		CNRM-CM5	CanESM2	IPSL-CM5A-MR	MIROC5		
2	YanOya	ACCESS1.0	ACCESS1.3	CNRM-CM5	CanESM2	IPSL-CM5A-MR			
3	MalwatuOya	ACCESS1.0		CNRM-CM5	CanESM2	IPSL-CM5A-MR		MPI-ESM-LR	
4	KalaOya	ACCESS1.0		CNRM-CM5	CanESM2	IPSL-CM5A-MR		MPI-ESM-LR	
5	DeduruOya	ACCESS1.0		CNRM-CM5	CanESM2	IPSL-CM5A-MR	MIROC5		
6	MaduruOya	ACCESS1.0		CNRM-CM5	CanESM2	IPSL-CM5A-MR		MPI-ESM-LR	
7	Kelani	ACCESS1.0		CNRM-CM5	CanESM2	IPSL-CM5A-MR	MIROC5		
8	KirindiOya	ACCESS1.0		CNRM-CM5	CanESM2	IPSL-CM5A-MR	MIROC5		
9	Mahaweli			CNRM-CM6	CanESM3		MIROC5	MPI-ESM-LR	GFDL-ESM2G

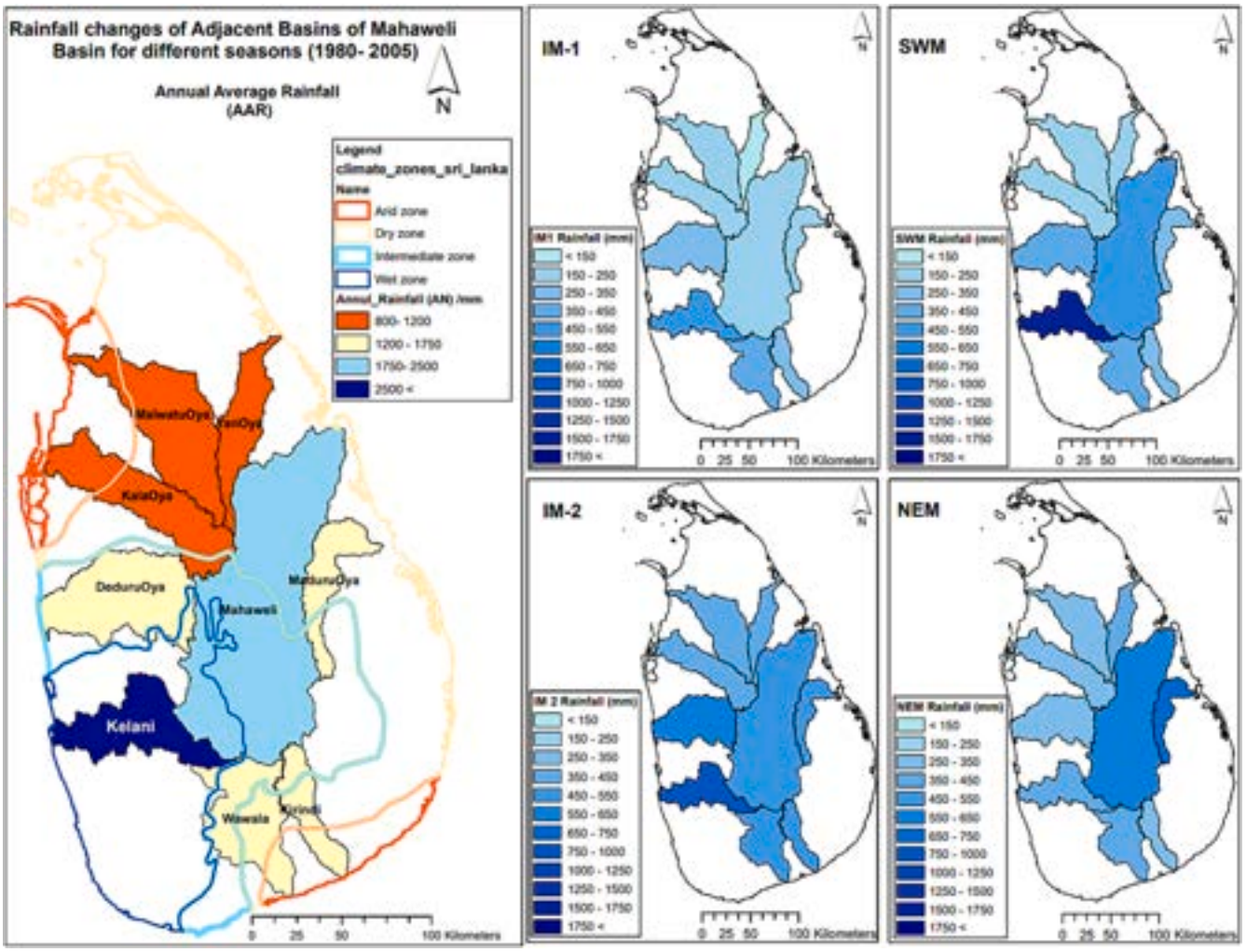

Fig. 7. Observed (1980–2005) average annual and seasonal (IM-1, SWM, IM-2, NEM) precipitation of the study area.

magnitude of WV between the reference reanalysis data and GCMs, as well as among GCMs, varied slightly. Yet, in both seasons, all selected GCMs reasonably represent the current climate for the Sri Lankan domain. As a result, all selected GCMs were confirmed to have good agreement with the current climate, producing consistent climatological patterns for both monsoons that are typical for our diverse study area and can be used for future climatological projection.

4.4. Future projections of seasonal and annual precipitation

Table 6 indicates the degree of difference (DOD) for GCM precipitation projections for the near future (NF), the middle future (MF), and the far future (FF) for all selected basins over four seasons and throughout the year with respect to the baseline period (1980–2005). According to the methodologies indicated in Section 3, the temporal and spatial outputs of the five GCMs for each basin were summarized. Spatial variations in the DOD of each basin are represented by the basin average. According to Table 6, ACCESS1.0 demonstrates decreased precipitation for nearly all seasons and regions in the near future. Furthermore, it indicates that most of the basins have a medium or high DOD (−25 %>) during NEM, whereas in the other seasons, all basins have a low DOD (<|−25 %|). CNRM-CM5 and CanESM2 have comparable patterns of DOD; however, their sensitivity varies significantly. Some GCMs have a low DOD variability for all seasons, whereas others

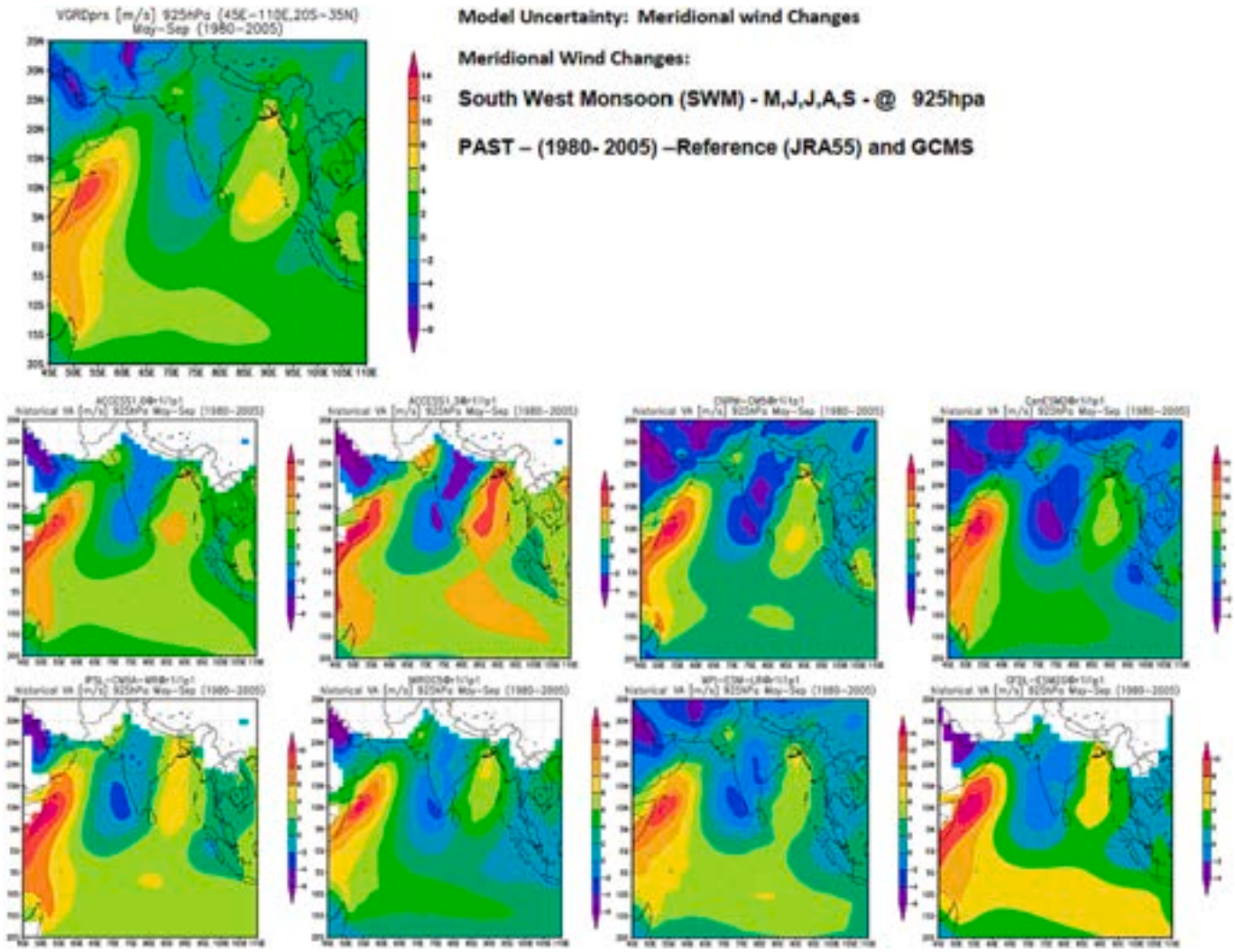

Fig. 8. Meridional wind of the current climate in m/s – SWM.

have a significant DOD variability. Annual DODs, on the other hand, are rather low. For example, CanESM2 provides a significantly higher DOD for SWM in all regions, presenting an increase in precipitation in the near future. Six GCMs show negative DOD for the IM-1 season, while the remaining two GCMs show increased DOD in all basins. The boxes are colored based on event sensitivity, with red or pink showing projections of decreased precipitation and light blue showing projections of increased precipitation. Additional information on the sensitivity of GCMs is provided at the end of this section.

Most of the GCMs show substantial changes in DOD (increased or decreased) for the middle-future (MF) precipitation projections when comparing the near-future DOD; however, CNRM-CM5 does not indicate significant changes in DOD (Table 6). Different seasons show various signals in GCM precipitation projections, some with a positive DOD and others with a negative DOD, implying an increase and decrease in future precipitation, respectively, compared to the baseline period. A few GCMs show the same increasing or decreasing trend during the same season or for a few seasons. For example, ACCESS1.0 for the Walawa and KirindiOya basins provided two different DODs; during IM-1 and NEM, precipitation is projected to be high and low decreases, respectively, while SWM and IM-2 seasons show a medium and low increase. CNRM-CM5 projects a moderate increase in precipitation (25 % $<$ DOD $<$ 50 %), which is projected to decrease in the near future, while both climatological periods for IM-2 anticipate a medium increase. The DOD for SWM is very high for CanESM2, which is more or less twice the DOD for the near future. Most of the DODs for all seasons increase for CNRM-CM5, MIROC5, and GFDL-ESM2G. Most of the GCMs indicated opposite behaviour (increases and decreases) in seasonal and annual DODs.

When comparing the DODs of NF and MF, all five GCMs show significant or high changes in DOD (increased or decreased) for the far-future (FF) precipitation projections (Table 6). The CNRM-CM5, MIROC5, and GFDL-ESM2G models show increased (positive) DOD for all seasons; however, the other GCMs show increased as well as decreased DODs, a mixed pattern over the seasons. Each GCM shows the same patterns for all basins over the seasons. CanESM2 shows a very high DOD for the SWM season, implying a higher precipitation increase. According to Fig. A.1, CanESM2 has a far coarser resolution than the other GCMs; thus, its projections may be overestimated due to the highly coarse resolution, and downscaling at the regional level may be less effective than other GCMs. As a result, there could have been a substantial difference. Because GCMs' resolution is substantially larger than the basin size, the signal may be overestimated or underestimated, dependent on the main bias correction and statistical-downscaling transform function. As a result, local climate change signals could not be captured effectively.

GCM sensitivities are classified as defined in Section 3. GCM sensitivities are shown as a palette on the appropriate event in Table 6. The blue color codes indicate an increasing trend, whereas the red color codes indicate a decreasing trend in relevant climatology (precipitation). The sensitivity of GCMs varies with the seasons. However, some of

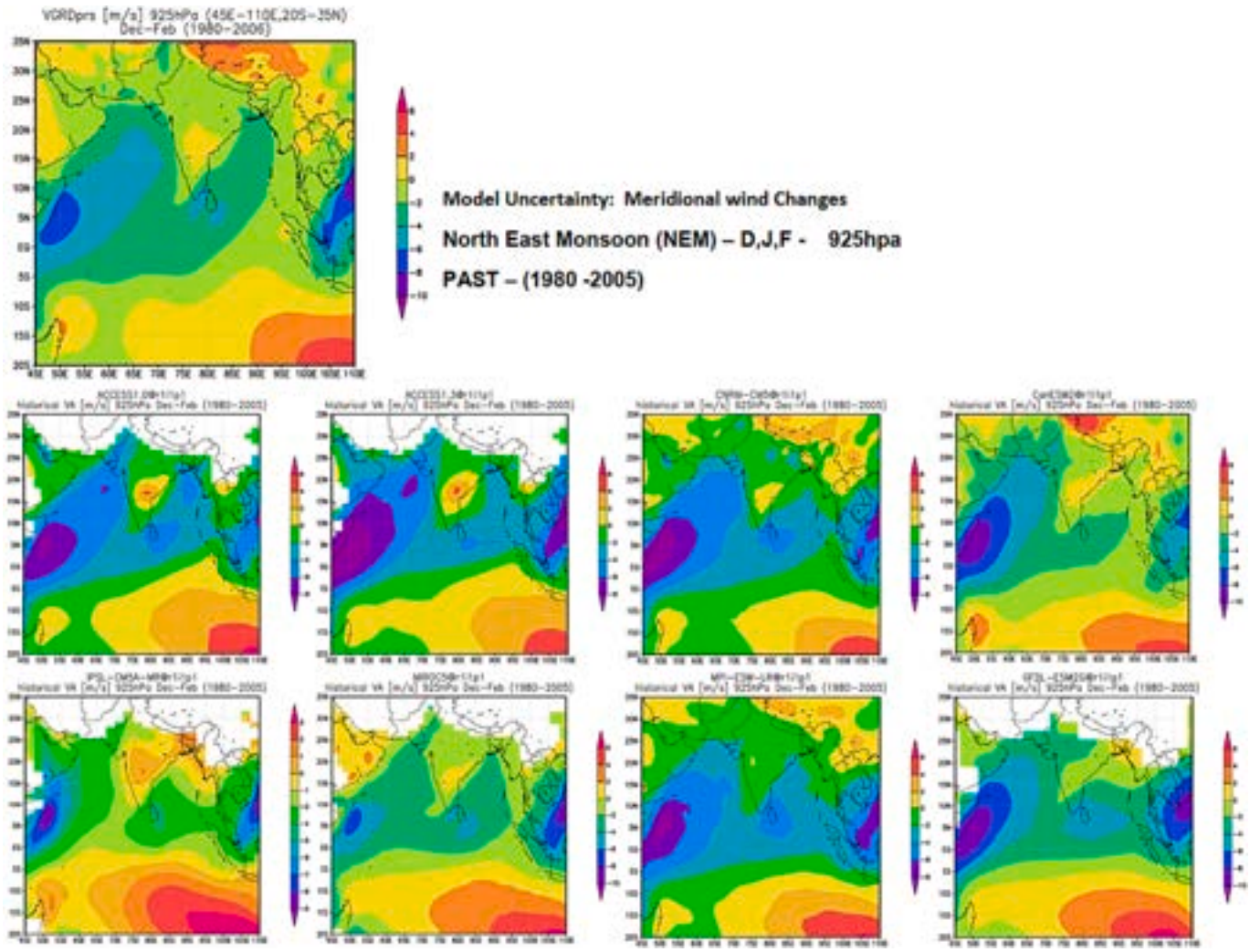

Fig. 9. Meridional wind of current climate in m/s – NEM.

the GCMs, such as CanESM2, show significantly higher differences, although most of the GCMs show high sensitivity over time, particularly in the far future.

4.5. GCMs uncertainty

The uncertainty analysis of GCMs is performed using the methodology given in Section 3 and takes into account the two monsoon seasons as well as the significantly affected climatological variables, meridional wind (MW) and wind vector (WV). The differences between future climatology and current climate (past climate (1980–2005)) were analyzed. As depicted in Fig. 10 the decrease (negative) in DOD for GCMs is linked to weak (−) meridional wind variations near the Sri Lankan domain during the SWM seasons. If meridional wind changes are strong (+) near the Sri Lankan domain during the SWM seasons, it causes an increase (positive) in DOD for most of the GCMs, as depicted in Fig. 10. Similarly, weak (-) meridional wind shifts near the Sri Lankan domain during the NEM seasons generate a decrease (negative) in DOD for GCMs, as depicted in Fig. 11. If meridional wind shifts are strong (+) in the Sri Lankan domain during NEM seasons, it leads to an increase (positive) in DOD for GCMs. Some of the GCMs, such as ACCESS1.0, CNRM-CM5, CanESM2, MIROC5, and MPI-ESM-LR, exhibit large MW changes over time (NF to FF), leading to significant DOD changes over time. At the same time, high MW fluctuations can be noted in the Somali jet, which intensifies SWM. Similarly to NEM, some of the GCMs, such as ACCESS1.0, CanESM2, and IPSL-CM5A-MR, exhibit substantial MW changes over time (NF to FF), resulting in significant DOD changes over time.

As depicted in Fig. 12, the decrease (negative) in DOD for GCMs is linked to weak wind vector (WV) variations near the Sri Lankan domain during the SWM season and vice versa. If WV changes are greater near the Sri Lankan domain during the SWM seasons, it causes an increase in DOD for most of the GCMs, as depicted in Fig. 12. Similarly, weak WV shifts near the Sri Lankan domain during the NEM seasons generate a decrease in DOD for GCMs, as depicted in Fig. 13. If WV shifts are strong in the Sri Lankan domain during the NEM seasons, it leads to an increase (positive) in DOD for GCMs. Some of the GCMs, such as ACCESS1.0, CNRM-CM5, CanESM2, MIROC5, and MPI-ESM-LR, exhibit large WV deviations over time (NF to FF), leading to significant DOD changes over time. At the same time, high WV fluctuations can be noted in the Somali jet, which intensifies SWM. Similarly to NEM, some of the GCMs, such as ACCESS1.0, CanESM2, and IPSL-CM5A-MR, exhibit substantial WV deviations over time (NF to FF), resulting in significant DOD changes over time. At the same time, considerable WV variations can be observed in ITCZ, which intensifies NEM.

GCM results differ for a variety of reasons, including GCM assumptions that simplify the climate system. The models simplify and make assumptions to be computationally manageable, but this introduces uncertainty into the results. Different GCM developers make assumptions and adopt various simplifications and boundary conditions, affecting the model projections. Small-scale phenomena that GCMs cannot resolve are represented via parameterizations. The results may

Table 6
Degree of Difference (DOD) precipitation for the near, middle, and far future.

Details of Basin					General Circulation Model Names (GCMs) NF(2025-2050) - Degree of Difference (DOD) Precipitation %																																			
No	Basin Name	Position with Mahaweli Basin	Basin Specified area	Relevant Climatic Zone	ACCESS1.0					ACCESS1.3					CNRM-CM5					CanESM2					IPSL-CM5A-MR					MIROC5					MPI-ESM-LR					GFDL-ESM2G				
					IM1	SWM	IM2	NEM	AN	IM1	SWM	IM2	NEM	AN	IM1	SWM	IM2	NEM	AN	IM1	SWM	IM2	NEM	AN	IM1	SWM	IM2	NEM	AN	IM1	SWM	IM2	NEM	AN	IM1	SWM	IM2	NEM	AN	IM1	SWM	IM2	NEM	AN
NF1	Walawa	South	BA	A,D,I,W	-6.6	-10	-3	-28	-10						-4	8.5	33	-0	12	-7	58.3	18	16	22	7.7	-13	4.7	33	6.7	5.4	9.9	4.8	15	9.2										
NF2	YanOya	North	BA	D	-22	-12	1	-26	-12	-29	-12	18	-2	2.6	6.8	16	25	3.6	15	-25	49.6	-2	-0	7.5	-7	0.3	6.8	8.8	6														
NF3	MalwatuOya	Northwest ,N	BA	D,A	-26	-14	1.9	-26	-11						-0	11	29	4.9	15	-16	50.4	3.8	2.5	10	-9	0.4	6.5	10	5.4						22	24	38	5.5	25					
NF4	KalaOya	Northwest	BA	I,D,A	-17	-16	0	-26	-12						-6	12	30	-0.1	12	-5	77.2	23	15	25	-4	-22	-2	21	0.7						22	22	39	3.2	24					
NF5	DeduruOya	West	BA	I,W	-9.4	-21	-2	-25	-12						-2	10	27	-0	12	-7	54.2	21	10	23	-3	-25	-5	26	-4	54	19	-3	14	13										
NF6	MaduruOya	East	BA	I,D	-7.3	-15	-4	-25	-13						1.2	13	19	-2	7.7	-3	87.1	19	16	26	4.3	-20	-1	8	0.9						10	23	37	2.7	20					
NF7	Kelani	West (upper)	BA	W	-9.9	-17	-1	-24	-12						-5	7.4	29	-1	9.9	-9	40.6	20	11	23	3.5	-14	1.4	31	-1	16	0.1	2.7	17	5.2										
NF8	KirindiOya	South	BA	A,D,I	-5.2	-4	-3	-29	-9						0.3	16	28	3	14	-6	72.1	19	18	25	11	-18	5.3	37	8.8	7.8	57	5	4.7	17										
NF9	Mahaweli	Own	BA	W,I,D											4.2	11	29	-8	9.6	-1	57	16	20	25						7.5	28	-7	14	11	13	6.9	46	22	25	-8	30	12	39	21

Details of Basin					General Circulation Model Names (GCMs) MF(2050-2075) - Degree of Difference (DOD) Precipitation %																																					
No	Basin Name	Position with Mahaweli Basin	Basin Specified area	Relevant Climatic Zone	ACCESS1.0					ACCESS1.3					CNRM-CM5					CanESM2					IPSL-CM5A-MR					MIROC5					MPI-ESM-LR					GFDL-ESM2G				
					IM1	SWM	IM2	NEM	AN	IM1	SWM	IM2	NEM	AN	IM1	SWM	IM2	NEM	AN	IM1	SWM	IM2	NEM	AN	IM1	SWM	IM2	NEM	AN	IM1	SWM	IM2	NEM	AN	IM1	SWM	IM2	NEM	AN	IM1	SWM	IM2	NEM	AN
MF1	Walawa	South	BA	A,D,I,W	-36	21	16	-11	2.7						-2	8.7	28	4.3	13	-23	126	41	-11	35	-19	-8	61	27	22	14	8.4	26	40	24										
MF2	YanOya	North (N)	BA	D	-19	28	-6	-15	-2	-28	-21	41	43	26	11	36	29	18	27	-19	70.5	-1	-25	3.4	-5	44	53	-4	31														
MF3	MalwatuOya	Northwest ,N	BA	D,A	-25	22	-4	-16	-4						8.1	35	32	19	27	-22	87.8	11	-23	10	-11	48	51	-2	30						-2	53	42	-12	27					
MF4	KalaOya	Northwest	BA	I,D,A	-30	16	2.4	-14	-3						7.7	18	28	13	20	-16	160	57	-15	38	-15	5.1	43	8.3	20						-1	44	43	-10	25					
MF5	DeduruOya	West	BA	I,W	-34	-1	8.3	-11	-4						9	15	27	13	19	-18	124	55	-24	43	-18	-16	38	15	11	71	21	12	40	27										
MF6	MaduruOya	East	BA	I,D	-30	18	6.3	-12	-1						14	25	23	8.4	19	-21	174	46	-12	33	-3	1.7	43	0.1	19						-7	59	41	-12	23					
MF7	Kelani	West (upper)	BA	W	-31	-6	8.9	-11	-5						0.6	8.3	28	6.7	13	-21	94.5	46	-19	47	-19	-14	47	25	8.7	32	-1.4	21	44	15										
MF8	KirindiOya	South	BA	A,D,I	-38	35	17	-11	6.2						0.3	15	26	3.2	15	-23	147	46	-10	37	-15	-6	60	27	27	7	51	30	16	29										
MF9	Mahaweli	Own	BA	W,I,D											6.7	20	35	0.3	16	-30	120	34	-25	27						35	35	23	16	28	0.6	33	39	-11	22	53	18	19	48	30

Details of Basin					General Circulation Model Names (GCMs) FF(2075-2100) - Degree of Difference (DOD) Precipitation %																																					
No	Basin Name	Position with Mahaweli Basin	Basin Specified area	Relevant Climatic Zone	ACCESS1.0					ACCESS1.3					CNRM-CM5					CanESM2					IPSL-CM5A-MR					MIROC5					MPI-ESM-LR					GFDL-ESM2G				
					IM1	SWM	IM2	NEM	AN	IM1	SWM	IM2	NEM	AN	IM1	SWM	IM2	NEM	AN	IM1	SWM	IM2	NEM	AN	IM1	SWM	IM2	NEM	AN	IM1	SWM	IM2	NEM	AN	IM1	SWM	IM2	NEM	AN	IM1	SWM	IM2	NEM	AN
FF1	Walawa	South	BA	A,D,I,W	-57	22	35	-11	5						-14	41	45	19	26	-32	160	71	-26	46	-17	7	87	84	44	51	18	37	85	44										
FF2	YanOya	North	BA	D	-69	28	14	-9	3	-40	-36	53	28	20	-5	98	45	22	44	-46	97	11	-34	7	-27	64	53	14	37														
FF3	MalwatuOya	Northwest ,N	BA	D,A	-66	14	15	-8	0						-10	91	51	21	42	-41	122	28	-32	17	-30	58	50	15	32						13	62	64	-21	39					
FF4	KalaOya	Northwest	BA	I,D,A	-63	8	16	-11	-4						-14	72	59	17	36	-24	209	88	-26	52	-37	14	64	29	30						10	52	64	-23	36					
FF5	DeduruOya	West	BA	I,W	-57	0.1	16	-14	-5						-13	57	55	19	36	-28	159	86	-33	59	-39	-18	66	38	20	162	68	33	82	66										
FF6	MaduruOya	East	BA	I,D	-57	21	15	-13	-2						0.1	74	41	20	33	-27	227	76	-22	45	-29	14	70	27	36						8	76	65	-20	36					
FF7	Kelani	West (upper)	BA	W	-52	-2	19	-13	-5						-16	32	44	20	26	-30	119	73	-33	60	-24	-13	71	70	19	80	8	37	94	35										
FF8	KirindiOya	South	BA	A,D,I	-59	36	37	-10	10						-14	55	43	21	29	-32	190	77	-23	49	-15	17	90	93	55	41	88	43	43	52										
FF9	Mahaweli	Own	BA	W,I,D											-7	62	45	19	33	-33	153	66	-28	42						99	77	36	67	63	23	49	75	-9	42	34	44	11	-42	7

Note:

Sensitivity

- Degree of Discrepancy of Rainfall increase (0 - 25 %)
- Degree of Discrepancy of Rainfall increase (25 - 50 %)
- Degree of Discrepancy of Rainfall increase (50% <)
- Degree of Discrepancy of Rainfall decrease (0 - 25 %)
- Degree of Discrepancy of Rainfall decrease (25 - 50 %)
- Degree of Discrepancy of Rainfall decrease (50 % <)

Area

BA : Basin Average
UB : Upper Basin
MB : Middle Basin
LB : Lower Basin

Climatic Zone

A : Arid Zone
D : Dry Zone
I : Inter-Mediate Zone
W : Wet Zone

Season (Months)

IM1 Inter mediate monsoon -1 (M, A)
SWM Southwest monsoon - (M, J, J, A, S)
IM2 Inter mediate monsoon - 2 -(O, N)
NEM Northeast monsoon - (D, J, F)
AN Annum - (J, F, M, A, M, J, J, A, S, O, N, D)

vary from one model to another because of the approximations and assumptions made in these parameterizations. Model developers' parameterizations can produce different outcomes. Further, these models use different numerical methods to solve climatic equations, which leads to varied model outputs. Similarly, GCMs use different spatial resolutions that directly impact the projections. The fine spatial-resolution models require more processing power, which limits simulations' temporal extents. GCMs estimate climate change based on several scenarios for greenhouse gas emissions. Due to the factors mentioned above, GCMs can give a variety of outcomes.

The uncertainty of GCMs is not only in the range but also in the direction (opposite direction, e.g., ACCESS1.0 and CanEsm2); this is caused by several reasons. An incomplete understanding of physical processes, limited processing power, and natural variability can cause climate model uncertainty. Even with the same initial circumstances and emissions scenarios, these uncertainties might affect model projections. Some models replicate stronger atmosphere–ocean feedback and greater warming, whereas others simulate weaker feedback and less warming. Natural variability also affects model projections. The complexity of the climate system and our understanding and computing power make climate models unreliable. When using model projections for decision-making, scientists must account for these uncertainties and continue research to improve our understanding and models (Mcfarlane, 2011; Randall et al., 2007).

Selvarajah et al. (2021)'s findings indicate that annual precipitation in the Mahawali basin is very likely to increase in the near future under the RCP8.5 scenario, which aligns well with our own findings (Table 7). Sirisena et al. (2021) found that under RCP 8.5 projections, the SWM in the Kalu River basin of Sri Lanka, located in the wet zone, may strengthen towards the latter decades of the 21st century, aligning with our results for far-future SWM projections (Table 7). Moreover, in the latest study on the climate projections of the central mountain region of Sri Lanka, ADB (2022) confirms that SWM precipitation projections would increase, while IM-1 precipitation projections would decline under the RCP8.5 scenario for the near future, which aligns with our findings (Fig. 14). Those results validate our findings at the respective river basins and regions. Our study shows that a seasonal-based analysis of uncertainty sources in climate change is necessary, rather than relying solely on an annual-based analysis, in accordance with the findings of Galavi and Mirzaei (2020).

Galavi et al. (2019) confirmed the importance of studying the impacts of climate change and uncertainty sources on smaller scales, such as seasonal scales, rather than solely focusing on decadal or annual scales. This aligns with our emphasis on small-scale factors (seasonal) in our decision-making matrix presentation, particularly in the context of water resources management.

4.6. *Future precipitation projection: GCMs for decision-making*

Future seasonal and annual precipitation probability trends for basins are illustrated in Fig. 14 using the methodology explained in Section 3. The largest basin, Mahaweli, indicates an extremely-likely increase in annual and SWM precipitation over time (NF, MF, and FF), whereas all western basins and the eastern side basin show the same more-likely-

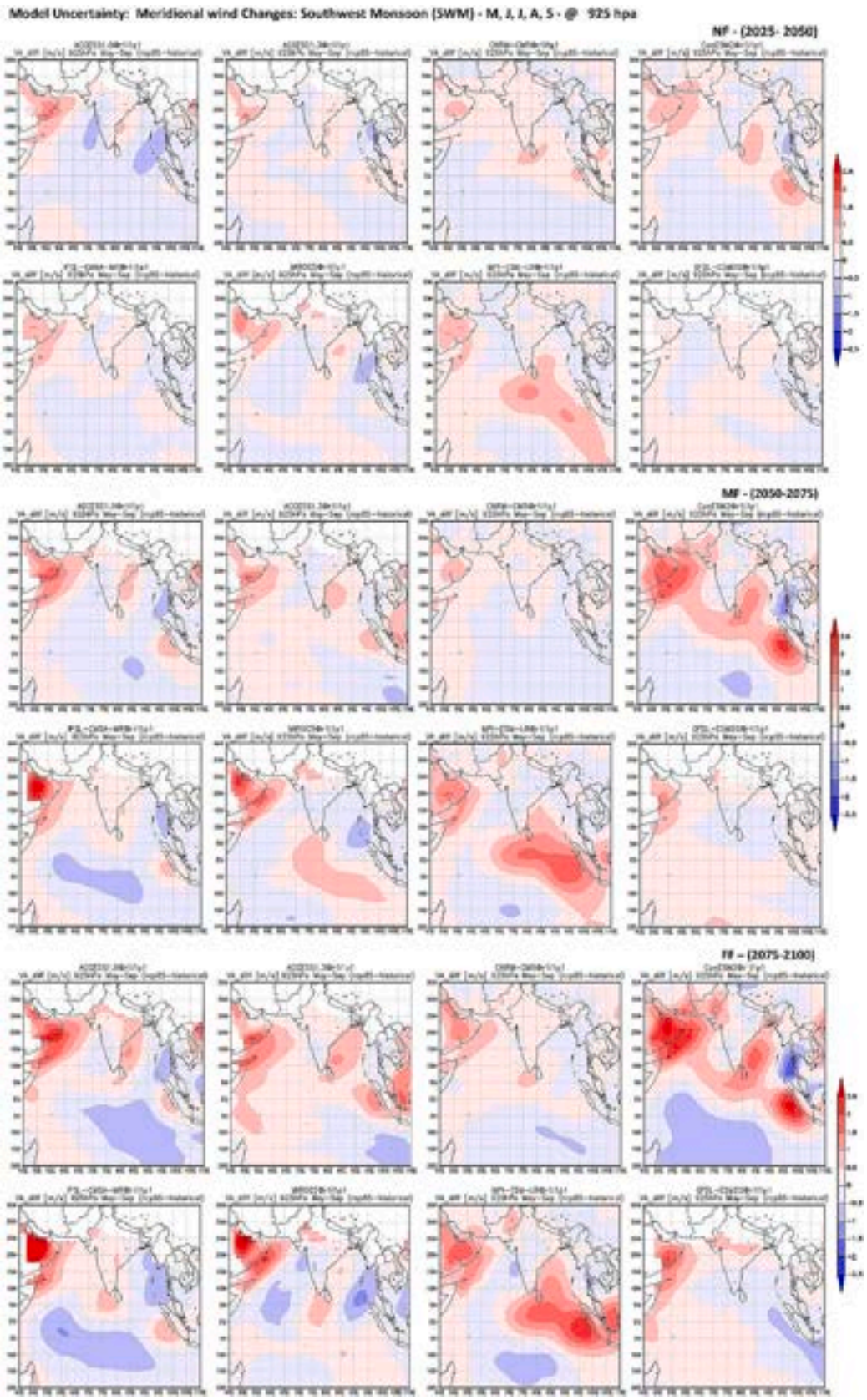

Fig. 10. Meridional wind changes for NF, MF, and FF for southwest monsoon (ACCESS1.0, ACCESS1.3, CNRM-CM5, CanESM2, IPSL-CM5A-MR, MIROC5, MPI-ESM-LR, and GFDL-ESM2G respectively).

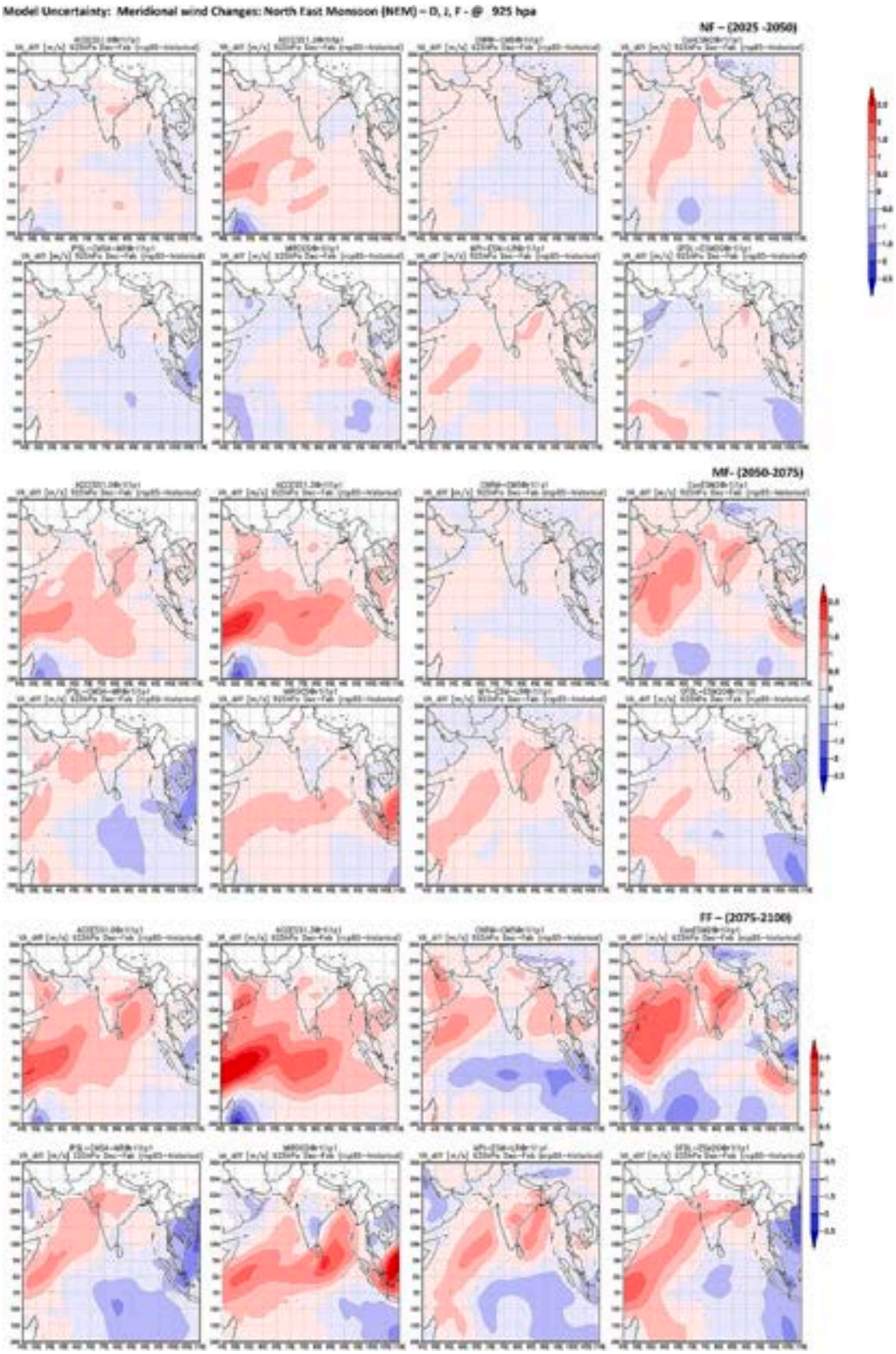

Fig. 11. Meridional wind changes for NF, MF, and FF for northeast monsoon (NEM).

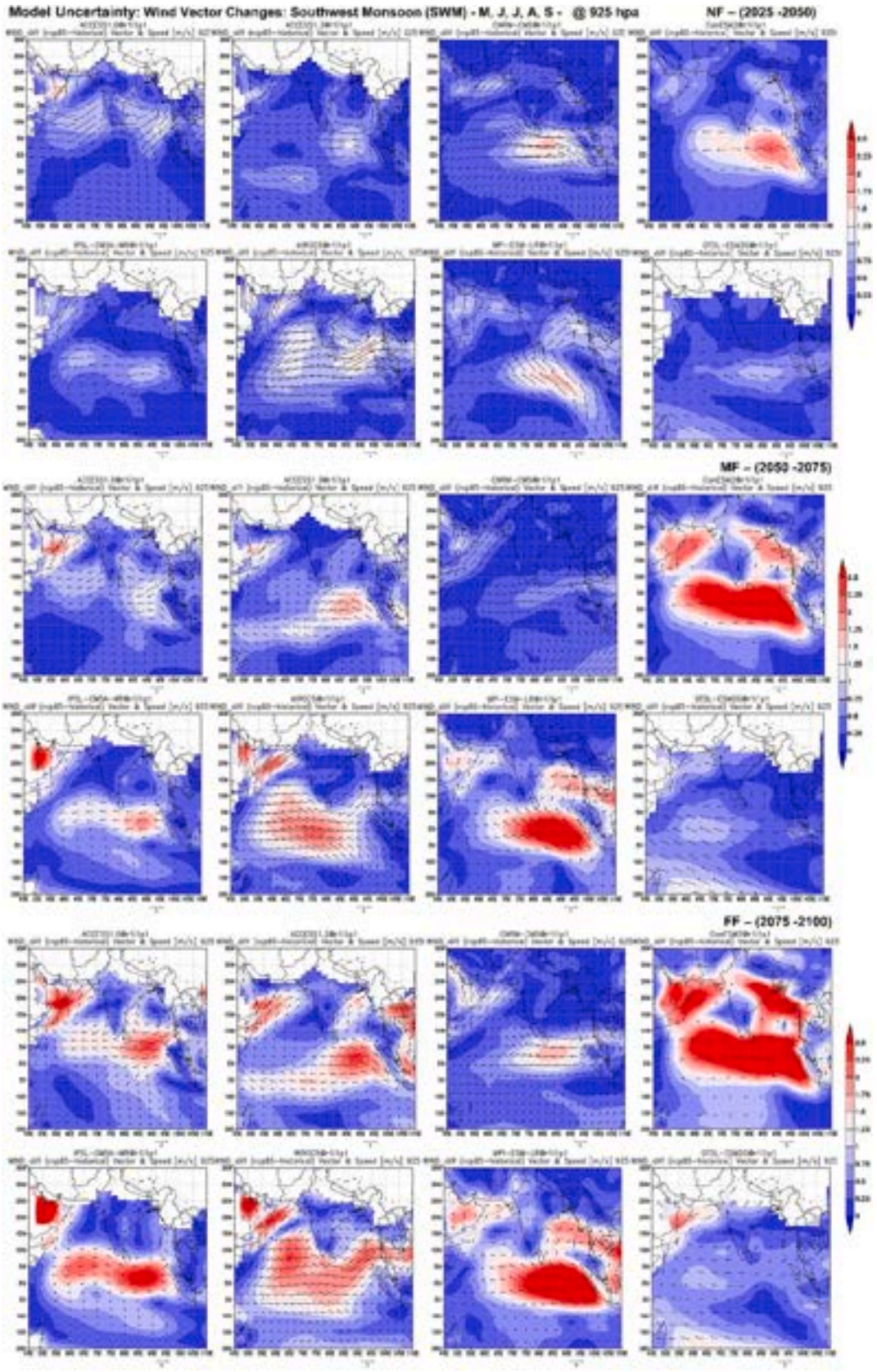

Fig. 12. Wind Vector changes for NF, MF, and FF for southwest monsoon (ACCESS1.0, ACCESS1.3, CNRM-CM5, CanESM2, IPSL-CM5A-MR, MIROC5, MPI-ESM-LR, and GFDL-ESM2G respectively).

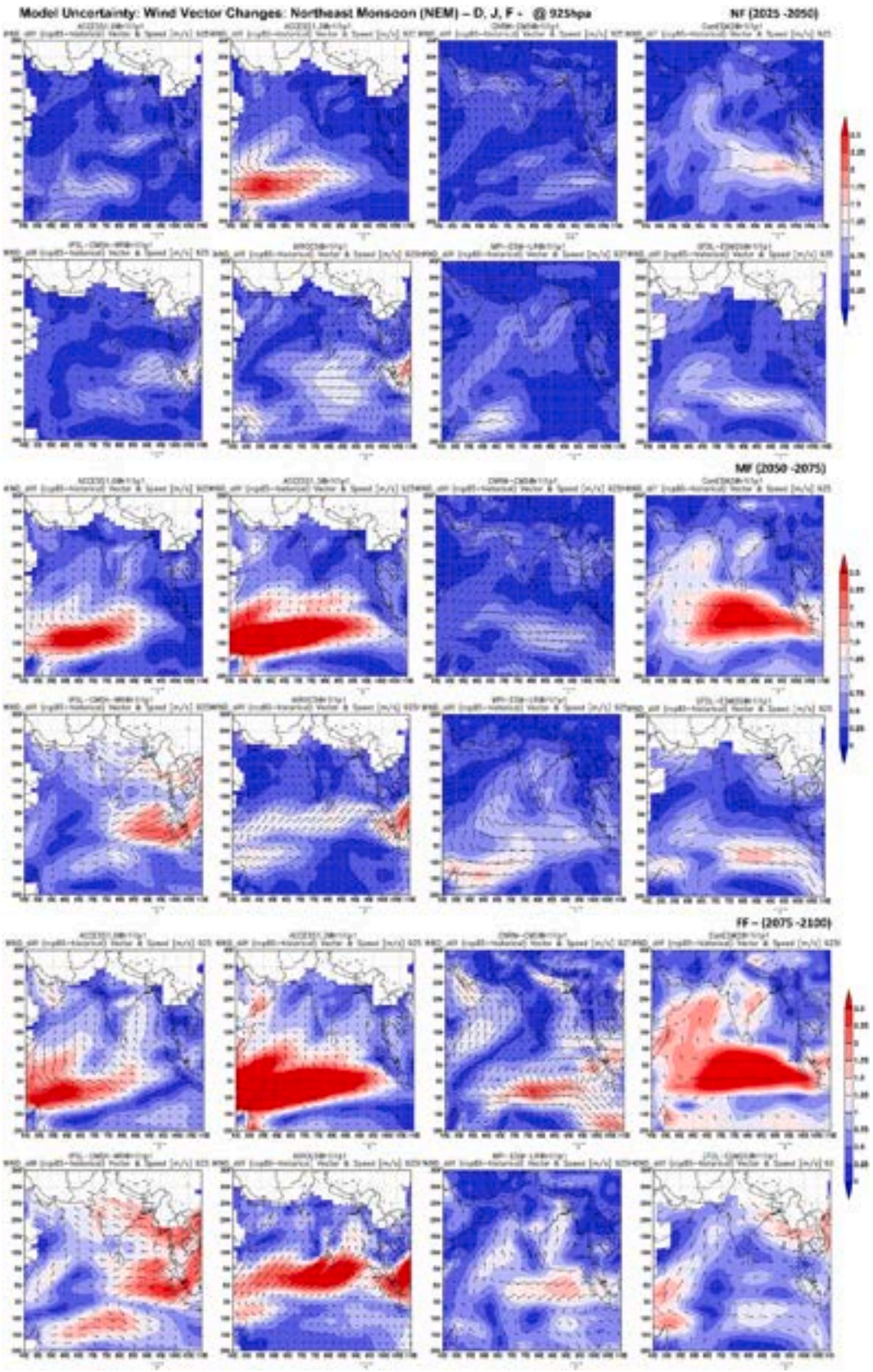

Fig. 13. Wind Vector changes for NF, MF, and FF for northeast monsoon.

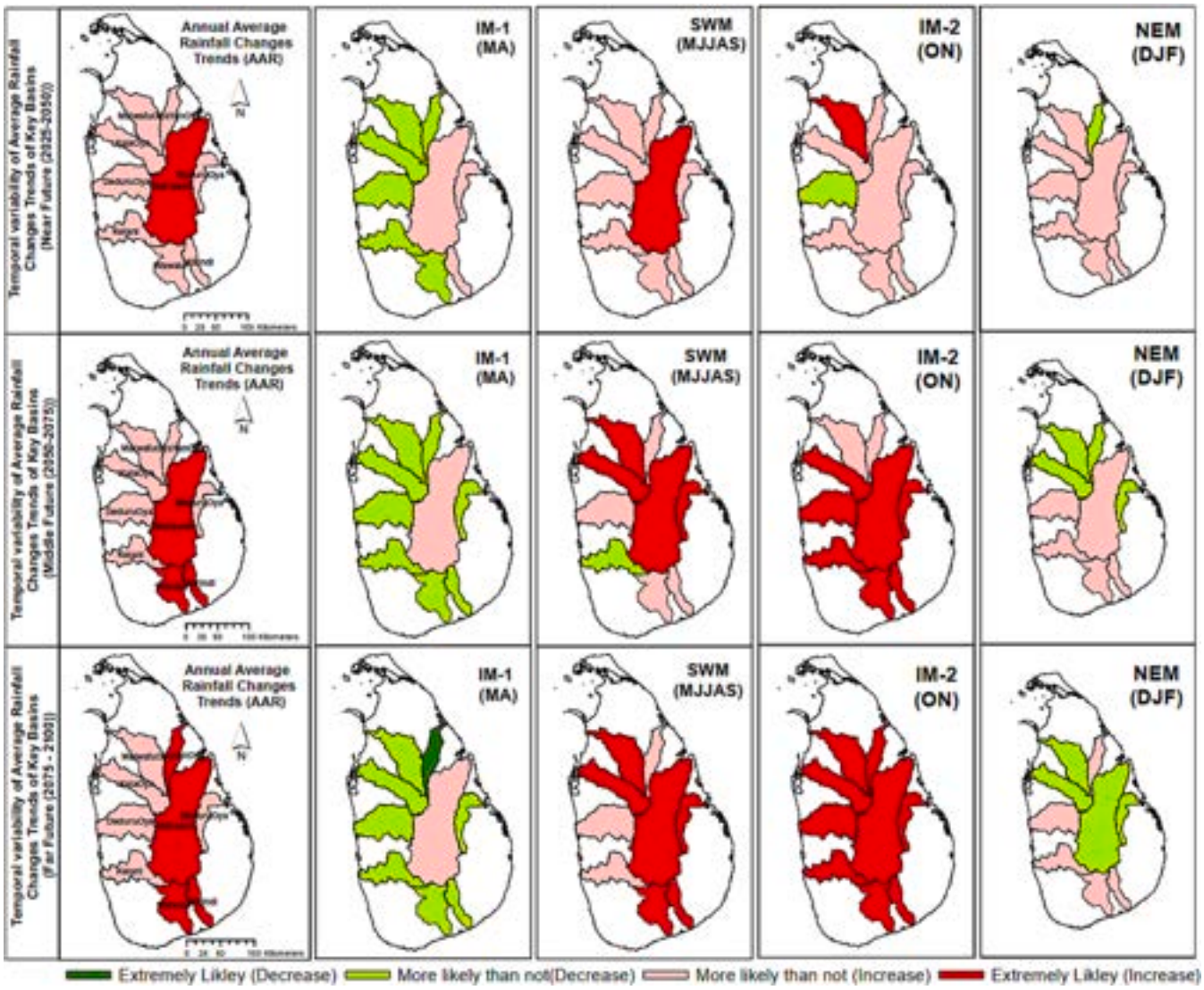

Fig. 14. Future seasonal and annual precipitation likelihood trend for basins.

than-not increasing trend. The southern basins showed an extremely-likely increasing trend for MF and FF though showing a more-likely increasing trend for NF. The YanOya basin is a narrow northern basin that is the only one entirely in the dry climate zone. It demonstrates a tendency that is more likely than not for NF and MF for annual precipitation, but extremely likely for FF. For the IM-1 season, all basins except Mahaweli, Kirindi, and MaduruOya display a more-likely-than-not decreasing tendency over time, but the Mahaweli basin shows a more-likely-than-not increasing trend over time. Similarly, most of the basins show an extremely-likely increasing trend in the IM-2 season for MF and FF, but the majority of the basins in NF show a more-likely-than-not increasing trend. Only the DeduruOya basin exhibits a more-likely-than-not decreasing trend for NF. For NEM, all basins show the same more-likely-than-not precipitation increasing trend except YanOya, which shows a decreasing trend. However, the northern and eastern basins show a decrease in precipitation for MF, and the Mahaweli basin also shows a decreasing trend for FF, while the YanOya basin exhibits an increasing trend. Apart from YanOya, all basins in NEM show a more-likely-than-not increase in precipitation. However, the northern and eastern basins have a decreasing precipitation trend for MF. The Mahaweli basin also has a decreasing precipitation trend for FF, while the YanOya basin has an increasing tendency.

4.7. C4 matrix for decision-making

Finally, our results are converted to a single decision-making matrix termed the C4 matrix (Table 7), which ultimately supports decision-making. It uses numerical values and color boxes to indicate the current observed and projected climate trends (NF, MF, and FF) for seasons and time periods for different basins. Critical confidences are based on a high degree of occurrence (more than 3 out of 5), and these red and light blue boxes represent the pertinent trends of occurrence events. The spatial and climate-zone details of each basin are specified in the first head column, and the current observed seasonal climate analysis details are summarized in the second. Each basin's defined climatic zones are confirmed with spatial variability observed in annual climate data and marked as colored box significance. The current climatic trend is depicted as a blue box (positive gradient) and a red box (negative gradient) as an increasing and decreasing trend, respectively. Reference regional and temporal likelihood trends according to the significance of the five selected GCMs for future climatic projections depicted in parallax. Moreover, we incorporated the simple average magnitude of the difference in seasonal and annual precipitations in the bottom row of the table relevant to the basin. This enables us to understand the average magnitude of future projections.

According to observed climate analysis (2nd head column, trend

Table 7
Color code climate change (C4) matrix for decision-making.

Details of Basins					INSITU (PAST)(1980-2005)					NF (2025-2050)					MF(2050-2075)					FF(2075-2100)				
					Average Rainfall (mm) / Climate Trend					Likelihood / Simple Average Magnitude % (DOD)														
No	Basin Name	Position with Mahaweli Basin	Basin Specified area	Relevant Climatic Zone	IM1	SWM	IM2	NEM	AN	IM1	SWM	IM2	NEM	AN	IM1	SWM	IM2	NEM	AN	IM1	SWM	IM2	NEM	AN
1	Walawa	South	BA	A,D,I,W	375	432	511	363	1674	2 -3	3 -2	4 -1	3 -1	4 -1	1 -4	4 -1	5 0	3 -2	5 0	1 -4	5 0	5 0	3 -2	5 0
					0.02	-0.02	0.00	0.01	0.00	-6	26	15	22	12	-20	41	34	24	19	-30	50	55	63	33
2	YanOya	North	BA	D	130	237	415	405	1178	1 -4	3 -2	4 -1	2 -3	4 -1	1 -4	4 -1	3 -2	2 -3	4 -1	0 -5	4 -1	5 0	3 -2	5 0
					0.04	0.01	0.03	0.00	0.02	-21	22	13	-9	8	-18	45	41	-14	22	-37	72	35	21	22
3	MalwatuOya	North West (North)	BA	D,A	169	210	419	326	1116	1 -4	4 -1	5 0	4 -1	4 -1	1 -4	5 0	4 -1	1 -4	4 -1	1 -4	5 0	5 0	2 -3	4 -1
					0.01	-0.02	0.02	0.00	0.00	-13	21	16	6	14	-15	49	34	-13	24	-37	70	42	-20	33
4	KalaOya	North West	BA	I,D,A	217	213	449	319	1190	1 -4	3 -2	4 -1	3 -1	4 -1	1 -4	5 0	5 0	2 -3	4 -1	1 -4	5 0	5 0	2 -3	4 -1
					0.01	-0.02	0.01	0.00	0.01	-8	37	23	13	15	-15	49	34	-13	26	-35	71	58	-20	39
5	DeduruOya	West	BA	I,W	291	443	558	257	1544	1 -4	3 -2	2 -3	3 -2	3 -2	2 -3	3 -2	5 0	3 -2	4 -1	1 -4	4 -1	5 0	3 -2	4 -1
					0.01	-0.02	0.01	0.00	0.00	-5	28	-3	17	16	-23	53	28	23	25	-34	71	51	46	45
6	MaduruOya	East	BA	I,D	176	261	484	718	1618	3 -2	3 -2	3 -2	3 -2	4 -1	1 -4	5 0	5 0	2 -3	4 -1	1 -3	5 0	5 0	2 -3	4 -1
					-0.01	-0.02	0.02	0.00	0.01	5	41	25	9	14	-15	56	32	-12	24	-28	82	53	-18	38
7	Kelani	West (upper)	BA	W	512	1715	848	382	3455	2 -3	3 -2	4 -1	3 -2	3 -2	2 -3	2 -3	5 0	3 -2	4 -1	1 -4	3 -2	5 0	3 -2	4 -1
					0.00	0.00	0.00	0.00	0.00	-8	10	13	20	13	-24	-7	30	25	21	-31	53	49	62	35
8	KirindiOya	South	BA	A,D,I	284	273	482	315	1347	3 -2	3 -2	4 -1	4 -1	4 -1	2 -3	4 -1	5 0	3 -2	5 0	1 -4	5 0	5 0	3 -2	5 0
					0.01	-0.01	0.01	0.01	0.01	6	48	14	16	16	-25	62	36	15	23	-30	77	58	53	39
9	Mahaweli	Own	BA	W,I,D	216	497	524	643	1863	3 -2	5 0	4 -1	4 -1	5 0	4 -1	5 0	5 0	3 -2	5 0	3 -2	5 0	5 0	2 -3	5 0
					-0.01	-0.02	0.01	0.00	0.00	8	27	26	24	18	24	45	30	22	25	52	77	47	-27	37

Note

Climate Zones

W	Wet Zone	> 2500 mm / Annum
I	Intermediate Zone	1750 - 2500 mm / Annum
D	Dry Zone	1200 - 1750 mm / Annum
A	Arid Zone	800 - 1200 mm / Annum

BA Basin Avarage

NF - Near Future, MF - Middle Future, FF- Far Future

Probability (likelihood) Occurrence Matrix	% Range	In case of five models
Extremely unlikely	0 - 5 %	0/5
More unlikely than likely	0 - < 50 %	(1/5,2/5)
More likely than not	> 50 - 100 %	(3/5,4/5)
Extremely Likely	95 - 100 %	5 /5

Seasons		Months
IM1	Inter Monsoon- 1	March-April
SWM	South West Monsoon	May - September
IM2	Inter Monsoon- 1	October to November
NEM	North East Monsoon	December to February
AN	Annual	January to December

Future Trend (agreement of 3 or more GCMs out of 5 selected GCMs) : Increase (+) Decrease (-)

gradient row), SWM is experiencing a declining trend, whereas other all-season climates (IM-2, NEM, IM-1) are experiencing a strengthening trend. It is highly confident that all the basins except Mahaweli will have a shortage of Inter-monsoon -1 (IM-1) precipitation in the future, while precipitation will increase during Southwest monsoon (SWM) and Inter-monsoon -2 (IM-2) in all the basins with some exceptions. An increase in NEM precipitation also shows in all the basins in the three periods considered except MalwatuOya, KalaOya, and MaduruOya in mid- and end-century periods (MF and FF). Furthermore, the largest basin, Mahaweli, also shows a decrease in NEM precipitation only in the far future. Overall, the majority of the GCMs show that annual precipitation will increase in all the basins.

The novel matrix presentation for climate data analysis offers several key merits. Firstly, it provides important basins' information, such as its location and climate condition, allowing for easy comparison and evaluation of regional climate variations. It contains historical climate variability data, which allows for a better understanding of how climatic patterns have changed through time in each basin and assists in identifying trends and patterns. The matrix presentation provides basin-specific climate projections for the near, middle, and far future, assisting stakeholders in anticipating potential climate changes and making informed decisions about adaptation and mitigation strategies. Additionally, it supports long-term planning and decision-making by considering future climate projections and helping politicians, researchers, and communities create plans and policies to deal with anticipated climate consequences. By displaying information on various basins, the matrix format promotes comparison analysis, assisting in finding similarities, variations, and regional trends in climate variability and projections.

This matrix structure, as seen in Table 7, is more beneficial for policymakers, particularly in analyzing both spatial and temporal distribution changes in precipitation. For example, precipitation reduces across basins except Mahaweli during the IM-1 season, requiring cautious water resource planning for agriculture and domestic needs. Similarly, during the NEM season, dry and wet zone discrepancies necessitate careful resource allocation, and temporal analysis demonstrates growing dryness during the MF and FF periods for the dry zone. This underscores the holistic value of this format for national water resource management. Therefore, the matrix's systematic and ordered format enhances accessibility and efficiently transfers complex climate data to diverse stakeholders such as policymakers, scientists, and the general public.

4.8. Decision making

Our study's key contribution is the introduction of a comprehensive approach to utilizing GCMs in decision-making. The C4 matrix (Table 7), based on the five principles and GCM outputs, can be utilized for decision-making. The use of the five principles confirmed addressing GCM uncertainty and spatial diversity to some extent. These five concepts can be used in any part of the world with diversity. If the GCMs resolution is high or well represents the study domain, the outcomes would be better. Policymakers and related stakeholders can utilize our C4 matrix to make more informed decisions on effective water resource planning (Viessman, 2008), disaster risk reduction (DRR), and fund allocations in the face of limited funds. Because of the simplicity of the C4 matrices, which were developed using cutting-edge scientific pieces of knowledge, not only the scientific community but also the general public can easily understand the matrix's content, and it could be used to send a reliable and reasonable message to nonscientific communities, such as politically motivated people. DRR can be addressed in two ways through the use of soft or hard countermeasures. These are mitigated measures, and other things include the implementation of structural and nonstructural measures to increase protection against disasters, such as floods and droughts (Dewald, 2011). The optimal design, planning, and implementation of structural and nonstructural measures to counteract disasters and reduce risks play a specific role. Furthermore, addressing design return periods and identifying risk-vulnerable areas in advance is vital in DRR. Our science-based C4 matrix provides the spatial and temporal variability (seasonal and long-term NF, MF, FF) of climate change effects (precipitation) that can be used to address the specified risk potentials and DRR in diverse regions.

5. Conclusions

This research presents a holistic approach to using GCMs in decision-making, focusing on the effects of climate change on precipitation while accounting for regional spatial and temporal variability in order to express scientific findings for establishing a decision-making support system based on five principles by addressing uncertainty in climate models, climate zones, and temporal change. The assessment is performed by 1) choosing and confirming competent GCMs based on their regional performance and current climate, 2) downscaling bias correction of climatological data for projecting future climatic data, identifying seasonal(4 seasons) and annual climate change signals for NF, MF, and FF, 3) identifying and evaluating the climatic sensitivity of GCMs, 4) understanding and clarifying the uncertainties of GCMs, 5) addressing the diverse regions (basin wise), and finally establishing a decision-making support system. Because of its diverse climate, we applied our methodology to Sri Lanka, covering nine key river basins as a case study.

Based on the performance in representing the current climate (1980–2005), high-performing GCMs were chosen for each basin, and it was discovered that the same set of GCMs was chosen for the same climatic zone. The four GCMs, i.e., ACCESS1.0, CNRM-CM5, CanESM2, and IPASL-CM5A-MR, were widely used in most of the basins analyzed. The current climate was captured adequately by each of the selected GCMs. The current climate pattern in terms of MW and WV was adequately reproduced by each of the selected GCMs; however, the magnitude of climatology in terms of MW and WV slightly varied. The GCMs have varying degrees of sensitivity, and sensitivity varies spatially and temporally. The degree of the climatology (precipitation) difference can be explained by the strength of the monsoons in the study area (large domain), and the strength of the monsoons can be described by variations in the meridional wind and wind vector.

GCMs provide significant and clear climate change signals for basins. Climate signals vary from season to season and year to year. As a result, it is not recommended to make judgments based exclusively on annual precipitation research, and incorporating seasonal climate is also critical for making better decisions on climate change. Each basin's average annual precipitation is likely to increase over the near, middle, and far future (2025–2100) under RCP 8.5 scenario; however, annual precipitation is extremely likely to increase in the Mahaweli basin (MB), the largest basin neighboring most of the other basins. Most of MB's surrounding basins show a more-likely-than-not decreasing precipitation tendency for inter-monsoon-1 in the future (2025–2100); however, MB shows a more-likely-than-not increasing trend. Our analysis shows that the observed climate SWM is declining, while the other all-season climates (IM-2, NEM, and IM-1) are strengthening. However, future climate projections show that SWM and IM-2 are more likely than not or extremely likely to strengthen, and NEM and IM-2 are more likely than not to weaken, excluding NEM in the near future. Adoption of simple detailed climate analysis charts could be more effective in expressing scientific messages to not only the scientific community but also the key actors among the general public who play a major role in consensus building and decision-making.

It is recommended that more GCMs ($n > 5$, where n is an odd number of GCMs) be used to evaluate future basin climatology projections in the interest of comparing the findings. Furthermore, in addition to the study of future projections of WV and MW climatological parameters, combined difference analysis of other significant climatological parameters (e.g., SST, SSP, T_{air}, and ZW) and El Nino-Southern Oscillation analysis would be recommended for a deeper explanation.

In the second stage of this research, we will analyze the spatial and temporal variations of future temperature projections. Furthermore, we will calculate future hydrological variability, considering temperature variations, by utilizing the water-energy budget-rainfall-runoff Inundation hydrological model (Rasmy et al., 2019) to provide a more comprehensive and detailed explanation.

6. Contributions

All authors contributed to the formulation of the research and the writing of the manuscript; S.I. developed the methodology, conducted the synthesis, analysed the model and observed the results, and wrote the manuscript. T.K. provided the necessary instruction, supervision, and review for the development of the research and the manuscript. H.S. gave inputs to develop the methodology and reviewed the manuscript.

Declaration of Competing Interest

The authors declare that they have no known competing financial interests or personal relationships that could have appeared to influence the work reported in this paper.

Data availability

Data will be made available on request.

Acknowledgement

The authors would like to thank the Public Works Research Institute (PWRI) and the International Centre for Water Hazard and Risk Management for providing the necessary research facilities. In this study, precipitation data provided by the Mahaweli Water Security Investment Program, Irrigation, and Meteorological departments of Sri Lanka was utilized. This dataset was also collected and provided under the Data Integration and Analysis System (DIAS), which was developed and operated by a project supported by the Ministry of Education, Culture, Sports, Science, and Technology. In addition, the DIAS system's tool resources were used for data archiving, processes, model simulations, and evaluation. The task was conducted with assistance from the JICA's long-term DRR Leaders Capacity Development program for the Sendai Framework. We also acknowledge the comments and suggestions made by anonymous reviewers that helped to enhance this manuscript.

Appendix A. Supplementary data

Supplementary data to this article can be found online at https://doi.org/10.1016/j.jhydrol.2023.130213.

References

Adb, 2022. Climate Change Risk Profile of the Mountain Region in Sri Lanka. Asian Development Bank. https://doi.org/10.22617/TCS220177.

Adler, R.F., Huffman, G.J., Chang, A., Ferraro, R., Xie, P.P., Janowiak, J., Rudolf, B., Schneider, U., Curtis, S., Bolvin, D., Gruber, A., Susskind, J., Arkin, P., Nelkin, E., 2003. The version-2 global precipitation climatology project (GPCP) monthly precipitation analysis (1979-present). J. Hydrometeorol. 4, 1147–1167. https://doi.org/10.1175/1525-7541(2003)004<1147:TVGPCP>2.0.CO;2.

Annamalai, H., Xie, S., Mccreary, J.P., Murtugudde, R., 2004. Impact of indian ocean sea surface temperature on developing El Niño. J. Clim. 18, 302–319.

Arumugam, S., 1969. Water Resources of Ceylon Sri Lanka. Water Resources Board, Colombo.

Central Bank of Sri Lanka, 2020. Key Economic Indicators. Recent Eonomic Dev. Highlights 2020 Prospect. 2021 2020, II–VIII.

Das, M., 2018. Journal of Climatology & Weather Assessment of Theissen Polygon Method to Analyse Monsoon Rain. J. Climatol. Weather Forecast. 6 https://doi.org/10.4172/2332-2594.1000241.

Dewald, van N., 2011. Introduction To Disaster Risk Reduction. Usaid 59.

Dierickx, F., 2019. Copernicus Climate Change Programme: User Learning Service Content. Uls.Climate.Copernicus.Eu 163.

D. Eckstein M.-L. Hutfils M. Winges BRIEFING PAPER, GLOBAL CLIMATE RISK INDEX 2019, Who Suffers Most From Extreme Weather Events? Weather-related Loss Events in 2017 and 1998 to 2017 2019 Greenwatch.

Galavi, H., Kamal, M.R., Mirzaei, M., Ebrahimian, M., 2019. Assessing the contribution of different uncertainty sources in streamflow projections. Theor. Appl. Climatol. 137, 1289–1303. https://doi.org/10.1007/s00704-018-2669-0.

Galavi, H., Mirzaei, M., 2020. Analyzing uncertainty drivers of climate change impact studies in tropical and arid climates. Water Resour. Manag. 34, 2097–2109. https://doi.org/10.1007/s11269-020-02553-0.

Gitz, V., Meybeck, A., Lipper, L., Young, C., Braatz, S., 2016. Climate change and food security: risks and responses. Food Agricult. Org. United Nations. https://doi.org/10.1080/14767058.2017.1347921.
Hannah, L., 2015. The climate system and climate change. Clim. Chang. Biol. 13–53 https://doi.org/10.1016/b978-0-12-420218-4.00002-0.
Hawkins, E., Sutton, R., 2009. The potential to narrow uncertainty in regional climate predictions. Bull. Am. Meteorol. Soc. 90, 1095–1107. https://doi.org/10.1175/2009BAMS2607.1.
IAS, P., 2016. Indian Monsoon Mechanism. PMF IAS 1–14.
IPCC, 2014. Climate Change 2014 Synthesis Report Summary Chapter for Policymakers. IPCC 31.
IPCC, 2013. Summary for Policymakers. In: Climate Change 2013: The Physical Science Basis. Contribution of Working Group I to the Fifth Assessment Report of the Intergovernmental Panel on Climate Change [Stocker, T.F., D. Qin, G.-K. Plattner, M. Tignor, S.K. Allen, J. https://doi.org/10.1260/095830507781076194.
IPCC, 2021. Summary for Policymakers. In: Climate Change 2021: The Physical Science Basis. Contribution of Working Group I to the Sixth Assessment Report of the Intergovernmental Panel on Climate Change [Masson-Delmotte, V., P. Zhai, A. Pirani, S.L. Connors, C. Péan, Cambridge University Press, Cambridge, United Kingdom and New York, NY, USA, pp. 3−32,. https://doi.org/10.1017/CBO9781139177245.003.
Kawasaki, A., Yamamoto, A., Koudelova, P., Acierto, R., Nemoto, T., Kitsuregawa, M., Koike, T., 2017. Data integration and analysis system (DIAS) contributing to climate change analysis and disaster risk reduction. Data Sci. J. 16 https://doi.org/10.5334/dsj-2017-041.
Kawasaki, A., Koudelova, P., Tamakawa, K., Kitamoto, A., Ikoma, E., Ikeuchi, K., Shibasaki, R., Kitsuregawa, M., Koike, T., 2018. Data integration and analysis system (DIAS) as a platform for data and model integration: Cases in the field of water resources management and disaster risk reduction. Data Sci. J. 17 https://doi.org/10.5334/dsj-2018-029.
Kobayashi, S., Ota, Y., Harada, Y., Ebita, A., Moriya, M., Onoda, H., Onogi, K., Kamahori, H., Kobayashi, C., Endo, H., Miyaoka, K., Takahashi, K., 2015. The JRA-55 Reanalysis: General Specifications and Basic Characteristics 93, 5–48. https://doi.org/10.2151/jmsj.2015-001.
Koike, T., Koudelova, P., Jaranilla-Sanchez, P.A., Bhatti, A.M., Nyunt, C.T., Tamagawa, K., 2015. River management system development in Asia based on Data Integration and Analysis System (DIAS) under GEOSS. Sci. China Earth Sci. 58, 76–95. https://doi.org/10.1007/s11430-014-5004-3.
Kotamarthi, R., Mearns, L., Hayhoe, K., Castro, C.L., Wuebbles, D., 2016. Use of Climate Information for Decision-Making and Impacts Research: State of Our Understanding. Prepared for the Department of Defense, Strategic Environmental Research and Development Program. Serdp Rep. 55.
Leung, L.R., T. Ringler, W.D.C., M. Taylor, and M.A., 2013. A Hierarchical Evaluation of Regional Climate Simulations. Trans. Am. Geophys. Union 94, 297–304. https://doi.org/10.1002/jame.20020.Neale.
Liebmann, B., Smith, C., 1996. Description of a complete (interpolated) outgoing longwave radiation dataset. Bull. Am. Meteorol. Soc. 77, 1275–1277. https://doi.org/10.4236/ojgas.2012.24042.
Mauritzen, C., Zivkovic, T., Veldore, V., 2017. On the relationship between climate sensitivity and modelling uncertainty. Tellus A Dyn. Meteorol. Oceanogr. 69, 1–12. https://doi.org/10.1080/16000870.2017.1327765.
Mcfarlane, N., 2011. Parameterizations : representing key processes in climate models. https://doi.org/10.1002/wcc.122.
Ministry of Mahaweli Development and Environment, 2016. National Adaptation Plan for Climate Change Impacts in Sri Lanka.
Moise, A., Wilson, L., Grose, M., Whetton, P., Watterson, I., Bhend, J., Bathols, J., Hanson, L., Erwin, T., Bedin, T., Heady, C., Rafter, T., 2015. Evaluation of CMIP3 and CMIP5 models over the Australian region to inform confidence in projections. Aust. Meteorol. Oceanogr. J. 65, 19–53. https://doi.org/10.22499/2.6501.004.
Moreira, L.F.F., Righetto, A.M., De Medeiros, V. m. a., 2006. Uncertainty analysis associated with rainfall spatial distribution in an experimental semiarid watershed, Northeastern Brazil. Proc. iEMSs 3rd Bienn. Meet. Summit Environ. Model. Software".
Nyunt, C.T., Koike, T., Yamamoto, A., 2016. Statistical bias correction for climate change impact on the basin scale precipitation in Sri Lanka, Philippines, Japan and Tunisia. Hydrol. Earth Syst. Sci. Discuss. 1–32 https://doi.org/10.5194/hess-2016-14.
Räihä, J., 2019. Do high and low climate sensitivity GCMs show differences in projected precipitation changes in Finland? FMI'S Climate Bull.: Res. Lett. 1 (1), 13. https://doi.org/10.35614/ISSN-2341-6408-IK-2019-01-RL.
Raisanen, J., 2001. Quantification of agreement and role of internal variability. J. Clim. 2088–2104.
Ranasinghe, E.M.S., 2010. Meteorological Setting of Sri Lanka. Environ. Dev. Sri Lanka – Vol. Felicitation Profr. Jayanthi Silva, Dep. Geogr. Univ. Colombo. Colombo. 1–9.
Randall, D., Wood, R., Bony, S., Colman, R., Fichefet, T., Fyfe, J., Kattsov, V., Pitman, A., Shukla, J., Srinivasan, J., Stouffer, R.J., Sumi, A., Taylor, K.E., 2007. Climate Models and Their Evaluation. IPCC Fourth Assess. Rep. Clim. Chang. 2007.
Rasmy, M., Sayama, T., Koike, T., 2019. Development of water and energy Budget-based Rainfall-Runoff-Inundation model (WEB-RRI) and its verification in the Kalu and Mundeni River Basins, Sri Lanka. J. Hydrol. 579, 124163 https://doi.org/10.1016/j.jhydrol.2019.124163.
Rayner, N.A., Parker, D.E., Horton, E.B., Folland, C.K., Alexander, L.V., Rowell, D.P., Kent, E.C., Kaplan, A., 2003. Global analyses of sea surface temperature, sea ice, and night marine air temperature since the late nineteenth century. J. Geophys. Res. 108 https://doi.org/10.1029/2002jd002670.
Sahu, N., Yamashiki, Y., Takara, K., 2010. Impact Assessment of IOD / ENSO in the Asian Region Impact Assessment of IOD / ENSO in the Asian Region.
Saroha, J., 2017. Indian monsoon: origin and mechanism. Int. J. Res. Anal. Rev. 4, 230–239.
Selvarajah, H., Koike, T., Rasmy, M., Tamakawa, K., Yamamoto, A., Kitsuregawa, M., Zhou, L.i., 2021. Development of an integrated approach for the assessment of climate change impacts on the hydro-meteorological characteristics of the mahaweli river basin, Sri Lanka. Water (Switzerland) 13 (9), 1218.
Shepard, D., 1968. A two-dimensional interpolation function for irregularly-spaced data. Proc. 1968 23rd ACM Natl Conf. ACM 1968, 517–524. https://doi.org/10.1145/800186.810616.
Sirisena, T.A.J.G., Maskey, S., Bamunawala, J., Coppola, E., Ranasinghe, R., 2021. Projected streamflow and sediment supply under changing climate to the coast of the Kalu river basin in tropical Sri Lanka over the 21st century. Water (Switzerland) 13 (21), 3031.
Smitha, P.S., Narasimhan, B., Sudheer, K.P., Annamalai, H., 2018. An improved bias correction method of daily rainfall data using a sliding window technique for climate change impact assessment. J. Hydrol. 556, 100–118. https://doi.org/10.1016/j.jhydrol.2017.11.010.
Solomon, S., D., Qin, M., Manning, Z., Chen, M., Marquis, K.B., Averyt, M.T., Miller HL, Solomon, S., Qin, D., Manning, M., Chen, Z., Marquis, M., Averyt, K.B., Tignor, M., Miller, H.L., 2007. Summary for Policymakers. In: Climate Change 2007: The Physical Science Basis. Contribution of Working Group I to the Fourth Assessment Report of the Intergovernmental Panel on Climate Change. D Qin M Manning Z Chen M Marquis K Averyt M Tignor HL Mill. New York Cambridge Univ. Press pp Geneva, 996. https://doi.org/10.1038/446727a.
T. Stocker Introduction to Climate Modelling 2016 (Universität Bern).
The national atlas of Sri Lanka, 2012. . Survey Department of Sri Lanka.
Thiessen, H., Alter, J.C., Thiessen, H., Tucker, F., Cole, H., 1911. Precipitation averages for large areas. Mon. Weather Rev. 39, 1982–1984.
USAID, 2015. Climate Change Information Fact Sheet SRI LANKA 2030, 1–4.
Viessman, W., 2008. Water resources planning and management. J. Contemp. Water Res. Educ. https://doi.org/10.1111/j.1936-704x.2008.00019.x.
Walker, W.E., Harremoës, P., Rotmans, J., van der Sluijs, J.P., van Asselt, M.B.A., Janssen, P., Krayer von Krauss, M.P., 2003. Defining uncertainty: A conceptual basis for uncertainty management in model-based decision support. Integr. Assess. 4, 5–17. https://doi.org/10.1076/iaij.4.1.5.16466.
WB, Adb,, 2020. Climate Risk Country Profile. Disaster Risk Reduct, Sri Lanka Status Rep, p. 2019.
WB, ADB, 2021. Climate risk country profile - Sri Lanka. Disaster Risk Reduct. Sri Lanka Status Rep. 2020 32.
Zhang, L.E.I., Xu, Y., Meng, C., Li, X., Liu, H., Wang, C., 2020. Comparison of statistical and dynamic downscaling techniques in generating high-resolution temperatures in China from CMIP5 GCMs. J. Appl. Meteorol. Climatol. 59, 207–235. https://doi.org/10.1175/JAMC-D-19-0048.1.